Master's thesis

NTNU
Norwegian University of Science and Technology
Faculty of Engineering
Department of Marine Technology

Carita Gyldenskog Ranvik

Simulation-based ship navigation for virtual testing of ship designs

Master's thesis in Marin Technology
Supervisor: Stein Ove Erikstad
June 2019

NTNU
Norwegian University of
Science and Technology

Carita Gyldenskog Ranvik

Simulation-based ship navigation for virtual testing of ship designs

Master's thesis in Marin Technology
Supervisor: Stein Ove Erikstad
June 2019

Norwegian University of Science and Technology
Faculty of Engineering
Department of Marine Technology

NTNU
Kunnskap for en bedre verden

NTNU
Det skapende universitet

Master Thesis in Marine Systems Design
Stud. Techn. Carita Gyldenskog Ranvik

"Simulation-based ship navigation for virtual testing of ship designs"

Spring 2019

Introduction

Improving ship energy efficiency means increased profit and reduced environmental impact. A simulation-based approach should therefore not be neglected in modern ship design. Proposed measures for GHG reduction and energy efficiency is optimizing ship design, deploying new energy efficient technology, and improving ship operation. No single measure is sufficient by itself. Due to the complex nature of ships and their operating context it is challenging to demonstrate the effect of potential design changes before vessels are built and brought into operation. The capital intensive and novel features of ship design have led to an industry being reluctant to utilise new technologies before it has been thoroughly tested. This creates a need to investigate how real operating conditions for vessels can be modelled virtually in a design context. Hence, we need to create realistic scenarios of ship behaviour under real weather conditions.

Background

Sandvik et al. (not published)[1] propose a model for generation of operational scenarios in which design evaluation of ships and ship systems can be performed using simulation. The novelty of their research is dynamic sea passage simulation. A depiction of ship transit is created by use of a mathematical representation of a captains decision-making process during sailing. The research is considered as part of the validation effort for models evaluating ship performance in waves by SFI Smart Maritime – WP 4. Their work illustrates the importance of considering sea passage scenarios in simulation-based design of ships.

Primary Objective

The primary objective is to develop more realistic and accurate simulations of sea passage voyages for application in simulation-based design of ships. By realistic we mean representing a voyage accurately and in a way that is true to life. This is achieved by combining vessel behaviour, operating context and dynamic navigational decisions in simulations. The candidate shall explore the external parameter influence on simulated performance and sailing pattern through comparison with full-scale data.

Scope of work

The candidate shall cover the following:

a. Provide a description of the problem
b. Present state of the art simulation applied as a tool in ship design
c. Describe a procedure to convert knowledge of marine technology into a simulation model
d. Develop a computational ship model based on available design data from a full-scale comparison ship forecasting ship behaviour
e. Validate the computational model against full-scale data
f. Implement the computational ship model to the sea passage model created by Sandvik et al. (not published)[1]
g. Explore and present insight on modelling features affecting operational performance in simulated sea passage scenarios

Implementation

Professor Stein Ove Erikstad will be the main supervisor from NTNU. PhD candidate Endre Sandvik will be co-supervisor. The work shall follow the guidelines made by NTNU for thesis work. The workload shall correspond to 30 credits.

Stein Ove Erikstad
Professor/Main Supervisor

[1] Sandvik, E., Nielsen, J.B, Asbjørnslett, B.E., Pedersen, E. & Fagerholt, K. (Not published), Scenario modelling of operational performance estimation.

Preface

This master thesis is written at the Department of Marine Technology at the Norwegian University of Science and Technology (NTNU) in Trondheim during the spring of 2019. The thesis is written as part of the Master of Science in Marine Technology with a specialisation in Marine Systems Design, and the work load is equivalent to 30 ECTS.

The focus of the thesis is to develop more realistic and accurate simulations of ship operation for application in simulation-based ship design. The thesis is based on sea passage simulator proposed by Sandvik et al. (n.d.) as part of the validation effort for models evaluating ship performance in waves by *SFI Smart Maritime - WP 4* (2019). The work is not published yet and therefore referred to with no date (n.d). Full-scale data used in this thesis is provided by *SFI Smart Maritime - WP 4* (2019) and results are made dimensionless in accordance with their guidelines.

I would like to thank Professor Stein Ove Erikstad for good guidance and discussions during this work. I would also like to express my gratitude and appreciation to co-supervisor PhD candidate Endre Sandvik. He has facilitated learning and contributed with highly valued inputs and opinions to this work. I would also like to thank my family for their encouragement and Hans Christian for his support throughout this degree.

Trondheim, 11.06.2019

Carita Gyldenskog Ranvik

Abstract

The primary objective is to develop more realistic and accurate simulations of sea passage voyages for application in simulation-based design of ships. To facilitate energy-efficient shipping, virtual proofing and validation of design concepts are central. Insight is provided on modelling of foreseeable weather horizon, delay cost modelling, and their effect on simulated sea passage scenarios. It is achieved through comparison of simulated sea passage voyages with full-scale data for a general cargo carrier. The presented work illustrates the importance of available information and decision making in simulation-based ship operations.

Impact on our understanding of ship system performance using simulation is assessed in a case study where two voyages are replicated over the North Pacific and compared to full-scale measurements. It is found that the ability to make strategic routing decisions is strongly dependent on available information with regards to weather forecasts. How the foreseeable weather horizon is modelled affects the selected route and encountered wave height significantly. For a forecasted weather horizon below 96 hours the simulated voyages go north of a storm situated on the great circle route, whereas the full-scale data showed that the human captain chose to go south of the storm and experience considerably lower wave heights. Depending on the delay cost model the simulated voyages sailed south for horizons of 96 hours and 102 hours, and experienced similar wave heights as the full-scale ship. This indicates that a human captain has a foreseeable weather horizon of at least 96 hours in this instance.

A study on delay cost modelling and its effects are also presented. Five different delay cost function forms are tested, and they display the ability to affect speed, path and strategic decisions. Strict delay cost models can affect the simulator to take strategic decisions early in a voyage. Two of the strictest delay cost functions manage to steer the simulated voyage south of the storm, with a six-hour shorter time horizon than the cost models that are less strict, and thus encounters calm seas and no delay.

Sammendrag

Hovedmålet med denne oppgaven er å utvikle mer realistiske og nøyaktige simuleringer for sjøkryssinger til implementering i simuleringsbasert skipsdesign. For å legge til rette for energieffektiv shipping, er virtuell validering av designkonseptet sentralt. Innsikt i modellering av værhorisont, forsinkelsesmodellering og deres effekt på simulerte sjøkryssinger er oppnådd gjennom sammenligning av simulerte seilas med fullskala data fra et cargo skip. Det presenterte arbeidet illustrerer betydningen av tilgjengelig informasjon og beslutningstaking i simuleringsbasert skipsoperasjon.

Konsekvensen av vår forståelse av systemets ytelse ved hjelp av simulering er vurdert i en case-studie hvor to reiser replikeres over det nordlige Stillehavet og sammenlignes med fullskala målinger. Det er funnet at evnen til å foreta strategiske avgjørelser er sterkt knyttet til tilgjengelig informasjon og da spesilet værmeldingen. Hvordan værhorisont er modellert påvirker den valgte ruten og erfart bølgehøyde betydelig. For værvarselslengde under 96 timer seiler den simulerte seilasen nord for en storm som ligger på den store sirkelruten, mens fullskaladataene viser at den menneskelige kapteinen valgte å gå sør for stormen og erfarte betydelig lavere bølgehøyder. Avhengig av kostmodellen for forsinkelse seilte de simulerte seilasene sør for stormen ved værhorisonter på 96 timer og 102 timer, og opplevde lignende bølgehøyder som fullskalaskipet. Dette indikerer at en menneskelig kaptein har en minimum værhorisont på minst 96 timer i dette tilfellet.

En undersøkelse av kostmodellering av forsinkelse og dens effekter presenteres også. Fem ulike kostmodeller for forsinkelse blir testet, og de viser at den har evnen til å påvirke fart, vei og strategiske beslutninger. Strenge kostmodeller for forsinkelse kan påvirke simulatoren til strategiske beslutninger tidlig i en reise. To av de strengeste kostfunksjonene for forsinkelse styrer den simulerte reisen sør for stormen, med en seks timers kortere tidshorisont enn kostnadsmodellene som er mindre strenge, og møter dermed roligere farvann og ingen forsinkelse.

Contents

List of Figures

List of Tables

Abbreviations

CFD	Computation fluid dynamics
EEDI	Energy efficiency design index
GHG	Greenhouse gas
GWP	Global warming potential
IMO	International maritime organisation
MCR	Maximum continuous rating
RANS	Reynolds-average NavierStokes equation
RPM	Revolutions per minute
OR	Operations research
SO	Simulation Optimizatin
FP	Forward perpendicular
H_s	Significant wave height
T_p	Spectral peak period
α	Wave propagation direction
CMA	Conditional modelling approach
hor	Horizon
κ	Delay cost rate
y_n	Cost function form
OD	Full-scale ship data
Fixed/fixed	Fixed calculations with ship model based on full-scale measurement's location and speed

Chapter 1

Introduction

From a global perspective environmental challenges in shipping needs to be addressed because it poses a threat to nature, human health and global warming (Eide et al. 2013). Carrying as much as 90 % measured in volume, shipping is the main carrier of world trade, providing an essential service to global economic development and prosperity (Smith et al. 2014). On average shipping accounts for approximately 3.1 % of annual global CO_2 emissions (Smith et al. 2014). If we are to meet the 50 % emission reduction target by 2050 set by International Maritime Organisation (IMO) energy efficient shipping is essential for reduction of GHG emissions. The mid-range forecast scenarios in the Third IMO GHG Study by Smith et al. (2014) show that by 2050, CO_2 emissions from international shipping could grow from 50 % to 250 %, depending on future economic growth and energy development.

"If we are to succeed in further enhancing the sector's energy efficiency, which is already the most energy-efficient mode of mass transport of cargo, the international community must deliver realistic and pragmatic solutions, both from technical standpoint and a political perspective". Smith et al. (2014)

1.1 State of the art

Improving the energy efficiency means increasing profit and reducing the environmental impact of shipping (Prpić-Oršić et al. 2016), and thus should not be neglected in the modern approach to ship design. Proposed measures for GHG reduction and energy efficiency is optimizing the ship's design, deploying new energy efficient technology, and improving ship operation (IMO 2011). Optimizing ship design can be done through reducing hull resistance, i.e. hull form and coating (Lindstad & Bø 2018, Prpić-Oršić et al. 2016, Zhang & Zhang 2018). New energy efficient technology can be machinery powered by alternative fuels (Lindstad 2018). Improvement of ship operation can be done through route and speed optimization

(Lu et al. 2015, Lindstad et al. 2013, Zaccone et al. 2018). In Bouman et al. (2017) a review of 150 studies published in literature are conducted to provide an overview of CO_2 reduction potentials and measures. The study indicates that no single measure is sufficient by itself if we are to meet the reduction targets in the Third IMO GHG study by Smith et al. (2014). Due to the complexity of ship design and its operations, it is a challenge to demonstrate the effect of potential design changes before vessels are built and brought into operation. Design performance is highly dependent on the operating profile of vessels, i.e. where, when and how they will sail. Traditional design methods typically do not include realistic operational aspects, but normally make simplified calculation based on an (assumed or estimated) average or representative condition (or limited number of conditions) for the operation (Fathi et al. 2013). With the rapidly developing technology and an increased computational capacity, it is now possible to integrate detailed subsystems of ship designs from various engineering disciplines into a system-based ship design process. This enables virtual proofing and validation of design concepts and reduces risk of not meeting design requirements (Skjong et al. 2017).

Simulation and optimization have been identified to be efficient tools in the task of virtual proofing and validation of design concepts. The capital intensive and novel features of ship design have led to an industry reluctant to utilise new technologies before it has been thoroughly tested (Skjong et al. 2017). The purpose of applying simulation-based design technology is therefore to lower risk, optimize design, reduce capital investment and ship development time as well as improve efficiency (Zhang & Zhang 2018). This creates the need to investigate how real operating conditions for a vessel could be modelled virtually in a design context, and how this effect the design process. To do this we need to create realistic scenarios of ship operation under real weather conditions. Ship operation in reality is highly influenced by heavy weather (Vettor & Guedes Soares 2015, 2016), and a captain attempt to avoid dangerous conditions and heavy storms. This task is traditionally dependent on a captain's experience and the weather forecast quality. Today the captain may also be assisted by weather routing systems integrated on board (Zaccone et al. 2018). Through stick and rudder commands the captain can alter speed and heading. The impact of human factors is difficult to capture and describe with mathematical models. If we can predict ship speed at any heading angle with respect to the current and future sea states, simulated ship operation under realistic conditions could be realised. Approaches relying on databases built on similar ships and AIS data have been used as scenarios in simulation (Bassam et al. 2015, Jalkanen et al. 2009). The relevance of historical data when other ship designs and time instances are in use must be investigated and has been questioned by Sandvik et al. (n.d.) and Lu et al. (2015). The performance of a ship in various conditions, i.e. fouling, speed, propulsion system degradation and draft conditions, may be different as well as the captain's operating policy and encountered weather.

1.2 Background

Sandvik et al. (n.d.) proposes a model for generation of operational scenarios in which design evaluation of ships and ship systems can be performed using simulation. The novelty of their research is dynamic sea passage simulation. A depiction of ship transit is created by use of a mathematical representation of a captain's decision process during sailing. The research is considered as part of the validation effort for models evaluating ship performance in waves by *SFI Smart Maritime - WP 4* (2019). Their work illustrates the importance of considering sea passage scenarios in simulation-based design of ships.

1.3 Objective

The primary objective is to develop more realistic and accurate simulations of sea passage voyages for application in simulation-based design of ships. By realistic we mean representing a voyage accurately and in a way that is true to life. This is achieved by combining vessel behaviour, operating context and dynamic navigational decisions in simulations. From comparison of simulated sea passage voyages with full-scale data, insight is provided on:

- Foreseeable weather horizon and its effect on simulated sea passage scenarios
- Delay cost modelling and its effect on simulated sea passage scenarios

1.3.1 Scope and delimitation

The study consists of:

- A presentation of relevant theory
- A presentation of the ship model
- Validation of a ship model through full-scale data provided by *SFI Smart Maritime - WP 4* (2019)
- Implementation of a computational ship model to a sea passage model created by Sandvik et al. (n.d.)
- Insight on simulated operational and tactical en route decisions

The sea passage model decision making process relies on the ability to forecast ship behaviour, thus great effort is put into validation of the ship model. It is also a purpose to increase the utility value for future research on this topic.

The limitations for this research are:

- The goal is not to verify ship design performance and operability. It is merely used as a learning basis to gain insight to simulated ship operations

- There were only available data for one vessel limiting the possibilities for validation
- Verification of ship design performance and operability is not the goal, the ship model's ability to predict ship behaviour only have to be considered accurate enough for the decision process in the sea passage model.
- Results are made dimensionless in accordance with guidelines given by the provider of the full-scale data, *SFI Smart Maritime - WP 4* (2019).

1.4 Thesis structure

This thesis consists of ten chapters. The first chapter consists of introduction and main objectives. In the second chapter research on how to assess ship design performance are presented and discussed. In the next chapters deep-sea vessel operation and appurtenant characteristics are presented, followed by modelling of ship operation. The case vessel used are presented in chapter five. In chapter six the model verification and validation study in relation to the computational ship model is presented followed by a case description, results, discussion and conclusion.

Chapter 2

Assessing ship design performance

Challenges with current practice are shortly discussed as well as tools for use in assessment of ship design performance. Ship design is complex, and it requires involvement of a wide range of engineering disciplines. Ship design has not been treated as an exact science but include a mixture of theoretical analysis and empirical data. Shipowners operate ships to make profit on their investment. Therefore, it is necessary to assess the environment and operating requirements to attain a feasible technical design that can operate economically and provide customer with a return on investment. The final design will often represent a compromise between conflicting interests, such as safety and energy efficiency. To reduce emissions and lower fuel consumption a smaller machinery may be installed, but with encounters of harsh sea it will be an unfortunate situation and thus a conflict in interests.

2.1 Design performance indicator

Design performance is of great interest to designers, ship owners and operators. With advancing technology and fierce competition between designers, accurate performance for ship evaluation has become more critical. Therefore, ship behaviour in real weather conditions has become a great interest for these three parties. Ship owners focus on reliable operation and high profit. Hence, accurate calculation of ship speed in real weather is essential from both economic and environmental aspects. The operator wants a safe ship having good sea capabilities i.e. reduced motions and slamming in high seas. Until now attention and effort have been focused on economy when designing new vessels. performance parameters such as fuel efficiency has been of interest. Due to environmental aspects new design performance parameters are emerging into the market. In 2014 the Energy Efficiency Design Index (EEDI) proposed by (IMO 2018) require future ship designs to be greener. Therefore energy saving and emissions reduction is the future of ship design development.

2.2 Simulation in ship design

Simulation and optimization have been identified to be efficient tools to virtually proof and validate design concepts. The capital intensive and novel features of ship design have lead to an industry reluctant to utilise new technologies before it has been thoroughly tested (Skjong et al. 2017). The purpose of applying simulation-based design technology is therefore to lower risk, optimize design, reduce capital investment and ship development time as well as improve efficiency (Zhang & Zhang 2018). This creates the need to investigate how real operating conditions for a vessel could be modelled virtually in design context and how this effect the design process.

2.2.1 Literature review

In Virtual Sea Trial by Simulating Complex Marine Operations (VISTA) by Erikstad et al. (2015), a framework for assessing a vessels performance over its life-cycle is introduced. It focuses on energy efficiency, improved operability and higher safety level. The challenge of interpreting how one component influences the system is addressed. In marine systems complex interaction between components are common. Therefore, making changes to one component will most likely affect other components as well, making it difficult to assess the exact effect. The same phenomenon is what complicates comparison between vessels. Improvements can be hard to attribute to a specific design choice. Virtual Prototyping of Maritime Systems and Operations (ViProMa) by Hassani et al. (2016) discuss issues regarding virtual prototyping in marine systems and operations. Three key factors for development of virtual prototyping framework is emphasised. It should be possible to compare concepts through relevant key performance indicators(KPI), e.g. fuel consumption. Assessing a vessels operability due to weather change with the use of Met-ocean data is of interest. The framework should also allow for change in main particulars and equipment installed. Hassani et al. (2016) suggest the use of black-box modelling and co-simulation to construct a system from stand-alone models. The black-box approach protect confidentiality regarding sensitive information. The drawback of such a method is lack of transparency. The result would be hard to verify, due to lack of knowledge. The simulation tool Gymir, developed by SINTEF Ocean in relation to SFI Smart Maritime is currently being validated. It is said to be an early-stage design assessment built to simulate an integrated ship system. Gymir simulates long-term performance of ships in realistic operation conditions. Effort has been put into validation of discrete-event simulation by (Sandvik et al. 2018).

Ship operation in reality is highly influenced by heavy weather (Vettor & Guedes Soares 2015, 2016) and a captain's attempt to avoid dangerous conditions in heavy storms. This task is traditionally dependent on the captain's experience and on weather forecast quality. Today the captain may also be assisted by weather routing systems integrated on board (Zaccone et al. 2018). Perera & Soares (2017) provide an overview of weather routing and safe ship handling approaches in the future

of shipping. Prpić-Oršić et al. (2016) propose a strategy for evolving eco-efficient green design by taking environmental issues into account during the design process. Jia et al. (2017) estimate the potential fuel savings and emission reductions attained through arrival requirements of ships in operation.

2.2.2 Optimization

Operations research (OR) applies advanced analytical methods to aid in the decision making processes. In relation to the maritime industry OR has been frequently used in ship routing and scheduling (Fischer et al. 2016, Christiansen et al. 2013). OR and computer science have developed discrete-event simulation software. Today optimization techniques of various kinds are frequently used in simulation practice. In ship design advanced optimization procedures are applied for sub-systems such as machinery and hull forms (Wang et al. 2014, Serani et al. 2016). A review of algorithms and the application of simulation optimization (SO) can be found in Amaran et al. (2014). When making a decision the intention is to optimize outcome. Optimization models are therefore applied to replicate decision processes. In Sandvik et al. (n.d.) an optimization for simulation approach to generate sea passage scenarios are presented.

2.2.3 Simulation and modelling review

Simulation can be defined as "the technique of imitating the behaviour of some situations by means of an analogous situation or apparatus to gain information more conveniently or train personnel" (Choi & Kang 2013). The former is known as analytic simulation and the latter as virtual environment simulation. In this study the focus will be on analytic simulation. Simulation can be used as a tool when experimenting with real-life systems is not feasible e.g. it is too costly to make a prototype, a real test involves too much risk or simply the situation is too complex to be handled mentally and we therefore need a computer to aid in simulating the situation. When building a simulation model, the system and appurtenant boundaries shall be well defined. Wu (1992) defined a system as "a collection of components which are interrelated in an organised way and work together towards the accomplishment of certain logical and purposeful end." State variables in a system plays a key role and can be defined as a particular measurable property of a system, e.g. queue length or service time of a system. A system where the state variables change continuously over time is called a continuous system, whereas a system in which state variables change instantaneously at discrete points in time is called a discrete-event system. The latter is relevant for this study. In discrete-event simulation the operation of the system is represented as a chronological sequence of events.

Top-down and bottom-up modelling

Top-down and bottom-up are both strategies for information processing. These methods are used in many contexts, such as ship design and LCA. A top-down

approach, also known as step-wise design, is essentially the breaking down of a system into sub-systems to gain insight in a reverse engineering fashion. This strategy is often used together with "black box" modelling. A bottom-up approach is the piecing together of systems to give rise to more complex systems. Hence, making original systems by emergent sub-systems. This modelling approach is for example used in system-based ship design. In the Third IMO GHG study by Smith et al. (2014) both top-down and bottom-up approaches is presented for the study.

2.3 Verification and validation

The concern of whether a model and its results are "correct" is addressed through model validation and verification. Model validation in this report is defined as "substantiation that a computerised model within its domain of applicability possesses a satisfactory range of accuracy consistent with the intended application of the model" (Schlesinger et al. 1979). Model verification is defined as "ensuring that the computer program of the computerised model and its implementation are correct" (Sargent 2004). The purpose and accuracy required of the model should be specified early in the development of the model. The validity of the model should be determined with respect to the purpose of the model. If it is a multipurpose model, the validity of the model should be determined with respect to each purpose. In Figure 2.3.1 a simplified version of the model development process from Sargent (1981) is displayed. The problem entity is the phenomena to be modelled; the conceptual model is the mathematical representation of problem entity; and the computerised model is the conceptual model implemented on a computer. In relation to this modelling process, the following definitions from Sargent (2004) are proposed:

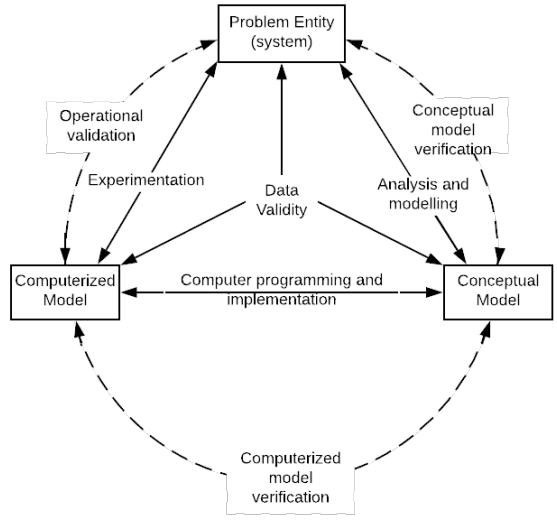

Figure 2.3.1: Modelling process from (Schlesinger et al. 1979, Sargent 2004)

Conceptual model validation: Determining if the theories and assumptions underlying the conceptual model are correct and the model representation of the problem entity is "reasonable" for the intended purpose of the model
Computerised model verification: Assuring that the computer programming and

implementation of the conceptual model is correct
Operational validation: Determining that the models output behaviour has sufficient accuracy for the models intended applicability.
Data validity: Ensuring that the data necessary for model building, model evaluation and testing are adequate and correct.

2.3.1 Validation techniques

This paragraph describes a selection of techniques and tests proposed by Sargent (2004) used in model verification and validation. The techniques can be used for validating and verifying the sub-models and overall model.

Comparison to other models: Outputs from valid models are compared to output from the simulation model, and through this the simulation model is validated. For this both analytic results and other simulation models can be used.
Degenerate test: The models behaviour is tested by appropriate selection of inputs and internal parameters in the model. For example, does the queue length increase when the arrival rate is larger than the service rate?
Operational graphics: Values of various performance measures are displayed graphically as the model runs through time. For example, a vessels location are visually displayed as the simulation model runs through time.
Sensitivity analysis: Through changing the inputs and parameters of the model the effect upon the models behaviour and output can be studied. By observing and comparing the relationships to real systems the model can be validated. The parameters that are sensitive, i.e., cause significant change in the models output, should be made sufficiently accurate prior to using the model (Sargent 2004).
Historical data validation: Historical data can be used to build and validate if the model behaves as the system.

Chapter 3

Deep sea vessel operation

Deep-sea shipping refers to the maritime transport of goods on intercontinental routes, crossing oceans. The main vessel categories in deep-sea shipping is oil tankers, container ships and bulk carriers. These three ship types is the most significant contributors from a CO_2 perspective, accounting for approximately 71 % of the CO_2 emissions from shipping and 75 % of the GHGs on a CO_2e basis (Smith et al. 2014). Common for all three vessel types are main engines primarily used for propulsion is the dominant fuel consumers. Deep-sea vessel operation profiles are typically dominated by the sea-passage, in laden and ballast condition. With long sailing distances on open seas segments such as time in port becomes small in comparison. The vessels are exposed to weather, different loading conditions and crew. Weather can potentially have a large impact on the ship resistance and consequently required power and speed. Required propulsion power increase in high wind and waves (Faltisen et al. 1980; Lloyd 1998) as opposed to calm-water conditions. By reliable speed reduction calculations, accurate prediction of required power, fuel consumption and emissions can be obtained. Journèe (1976) introduced a method for voluntary speed reduction and the behaviour of the ship in a sea-way with head weaves. Prpić-Oršić & Faltinsen (2012) developed a method for estimating attainable speed in moderate and severe sea, based on the Beaufort scale. Lu et al. (2015) proposed a semi-empirical ship operational performance prediction model based on Kwon (2008).

3.1 Characteristics

Simulating a ship in operation requires a comprehensive modelling effort. The ship must be broken down into subsystems, and modelled at a fidelity level sufficient for representation of the real system. Overall, the system contains exogenous factors having an external cause or origin. It also contains endogenous factors having an internal cause or origin. Further it is divided into a physical domain containing the ship and occurring weather. In the operational domain operation/ship owner

and weather forecast is placed. The captain is placed as an interface between the physical and operational domain, converting mission constraints given by the ship owner to navigational commands at sea, Sandvik et al. (n.d.). In the following subsections, the different components are described.

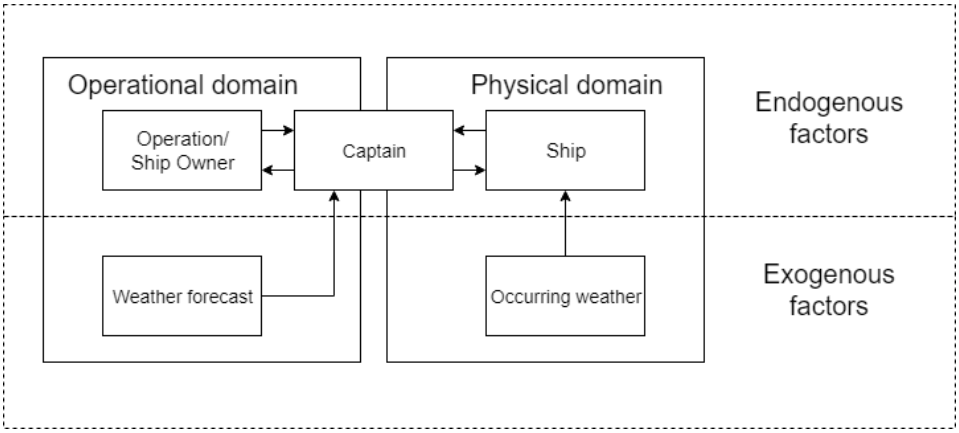

Figure 3.1.1: Visualisation of operational simulation for ships Sandvik et al. (n.d.)

3.1.1 Environment

Weather factors relevant for ship operation is; waves, wind, current, sight and tides. A met-ocean model is required to describe characteristics of environmental loads and corresponding variability in ship system performance. Hindcast wave data is available from the *European Centre for Medium-Range Weather Forecast* (2018). In Janssen & Bidlot (2018) operational sea state forecasting module spectra is verified against observed spectra by buoys. It shows a clear reduction in wave height scatter index in particular for short range forecast up to 5 days ahead.

3.1.2 Captain

Operation of a vessel is controlled by the crew onboard. How the crew operates the vessel is subjective and influence by weather conditions and experience. In storm and heavy seas, the ship's captain will most likely voluntarily reduce ship speed to reduce slamming, excessive accelerations and propeller racing. This is what is referred to as voluntary speed reduction. The behaviour of the captain in specific circumstances is subjective and depends on the captain's experience and abilities. Consequently, it is difficult to predict and capture real behaviour in a simulation. Another aspect of the voluntary speed loss is modelling of engine dynamics, i.e. how the engine responds to inputs. In real systems a time delay will be experienced due to inertia of the system. To capture this accurately in models is a complex task. Involuntary speed loss is due to increased resistance from wind and waves. The ship motion and added resistance increase the work load on the propulsion

system and results in increased fuel consumption and speed loss (Prpić-Oršić & Faltinsen 2012).

3.1.3 Operation/ship owner

Ship owners and operators strive to lower cost. For deep-sea vessels the fuel cost is a major part of the operating budget. There is said to be three basic modes of operation; Industrial Shipping, Tramp Shipping and Liner shipping. In industrial shipping the cargo owner controls the fleet and the objective is to ship the total demand whilst minimizing cost. In tramp shipping we find a combination of contracted cargo and optional spot cargoes. The ship follows the available cargo similar to a taxi service. The objective is to maximize profit by selecting optimal spot cargoes. In liner shipping the ship follows a published schedule similar to a bus line. Liner shipping includes container, RoRo and general cargo carriers. Common for industrial shipping, tramp shipping and liner shipping is that route and scheduling is very important to stay profitable. At the freight market sea transport is bought and sold. There are four types of contractual agreement that are commonly used (Stopford 2009):

1. Voyage charter: The ship owner commits to carry a specific cargo for an agreed up-on price per ton that cover all expenses
2. Contract of affreightment: The ship owner commits to transport a regular tonnage of cargo for a agreed price per ton, covering all cost
3. Time charter: The ship with crew is hired for a fee per day, month or year. The ship owner is responsible for paying capital cost and operating expenses whilst the charter party pay the voyage cost
4. Bare boat: This is in reality a financial agreement, where the ship is hired without crew or any operating responsibilities.

To optimize ship/fleet operation various operation strategies are applied. Common for all ship owners and operators is that they want to deliver in accordance with the contract, thus time window for cargo delivery and pick-up, and knock-on effect affecting future vessel and fleet operation should be considered in the design process.

3.1.4 Ship

The ship model allows estimates of power and fuel consumption for a given location, weather conditions and ship speed. Such a model requires:

- Hydrodynamic resistance calculations
- Propulsion and machinery performance prediction
- Seakeeping performance

In the following sections theory is presented on these topics.

3.2 Hydrodynamic resistance

Ship resistance calculation is a complex task. This is because resistance of a ship does not originate from only one source, but many.

3.2.1 Resistance components

Total resistance R_T consists of calm water resistance R_{T0} and added resistance due to waves R_{AW} and wind R_{AA}.

$$R_T = R_{T0} + R_{AW} + R_{AA} \tag{3.2.1}$$

The calm water resistance term is weather independent and added resistance are influenced by weather conditions and relative direction.

Resistance components in calm water

The following text is based on (Amdahl et al. 2013) and (Steen & Minsaas 2014). The total resistance is commonly divided into viscous resistance and residual resistance (Amdahl et al. 2013). The viscous resistance and residual resistance can further be divided as seen in Figure 3.2.1.

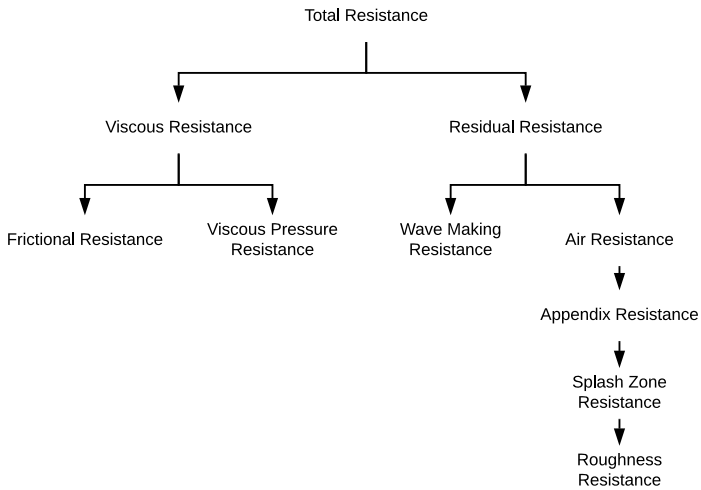

Figure 3.2.1: Calm water resistance components based on (Amdahl et al. 2013)

Frictional resistance: When a ship slide through water the water particles in contact with the hull will stick to the hull. They do not get any relative motion to the ship. This is called the "no-slip"- boundary condition. Because of this phenomenon, the relative velocity of the water particles to the ship will increase with increasing distance from ship. This gives a shear force along the ship hull,

and this shear force is what we call frictional resistance. The frictional resistance constitutes a significant part of the total resistance due to the ships wetted surface, and it is strongly affected by ship speed.

Viscous pressure resistance: Viscous pressure resistance is a result of pressure to viscous effects mainly due to relief of flow from hull.

Wave making resistance: When a ship moves in the water surface waves are generated. Waves contain energy, and this energy comes from the ship. To move in the water surface more energy have to be used than if there were no wave making resistance. The formation of waves is therefore a counter force to the ships movement. The wave making resistance can further be subdivided into wave reaking resistance and wave pattern resistance. The wave making resistance is the largest contributor to the residual resistance. By use of a bulb that is positioned correctly according to the ships wave system, the wave making resistance of the whip will be reduced.

Air resistance: The air resistance is a result of air being pushed against the superstructure of the ship. Air resistance is a result of the ships speed.

Other resistance components: The appendix resistance arises due to bilge, rudders, shafts, tunnel thrusters and other equipment necessary but has a negative effect on hydrodynamic hull shape. Splash zone resistance is a result of water spray that arises when the ship moves. This component is more dominating on speedboats and is normally found in the bow area. It is very hard to measure this component.

Roughness resistance: Roughness of a surface will increase the frictional resistance between the surface and the environment. Increased roughness in the hull surface arise due to e.g. damages in the coating, corrosion, and fouling. A large roughness on the submerged area of the hull can have a large impact on the total resistance and result in significant increase in operational costs. An increase of roughness over time is expected and is affected by maintenance frequency. Fouling of marine organisms are a commonly known problem, and coatings to reduce this has been developed. These coatings can have a negative effect on the ocean environment, due to its content, (Amdahl et al. 2013).

Added resistance due to waves

Added resistance due to waves are a result of interaction between the ship and incoming waves. It can be divided into two physical phenomena; wave reflection and vessel motion induced wave generation.

Added resistance due to wind

Added resistance due to wind is a result of the relative velocity between wind and ship. The ships superstructure will influence the size of this term. For ships with small superstructures, it is not unusual to neglect this component, (Amdahl et al. 2013).

3.2.2 Ship resistance modelling review

Ship resistance prediction is used in prediction of required propulsion power, that in turn is used for calculation of propeller thrust, which is critical in terms of propeller selection. Accurate ship resistance prediction is elusive due to the three-dimensional flow pattern around the hull. In Tillig et al. (2018) a generic energy ship system model for design and operation of ships is presented and demonstrated in a simulation case study for a Panamax tanker. Steen & Minsaas (2014) divide resistance calculations methods into three categories:

1. Empirical methods
2. Numerical methods
3. Experimental methods

Empirical methods

Methods developed in this category are based on "old fashioned" hull shapes that are not in use any more. Over the last 30 years energy saving hull shapes has been developed, therefore these methods predict too high resistance. The main problem with the methods are that they do not consider the bulb in a satisfactory way. Ships today are commonly equipped with bulb. Another weakness with these methods are not accounting for details in the ship-frame. In Steen & Minsaas (2014) it is stated that the two most important parameters in ship resistance estimation are the fullness and Froude's number. It is observed that the resistance increases rapidly after a certain speed for all ships. Hence, the service speed is placed well below this point.
The most resent published empirical method for empirical resistance prediction of conventional ships is Hollenbach (Steen & Minsaas 2014). Only models tested later than 1975 where considered in his study. Hollenbach's methods is the most precise method among this types of methods, Table 3.2.1. Holtrop & Mennen (1982) is a result of the most extensive static analysis of models test results ever made. It is not as accurate as Hollenbach, but widely used.

Table 3.2.1: Comparison of empirical resistance predictions methods from Steen & Minsaas (2014)

	Single-screw design draft		Single-screw ballast draft		Twin-screw design draft	
	Mean	Standard deviation	Mean	Standard deviation	Mean	Standard deviation
Holtrop-Mennen	-0.5 %	12.8 %	6.3 %	16.1 %	5.8 %	18.4 %
Guldhammer	0.8 %	11.0 %	10.5 %	17.9 %	11.2 %	19.2 %
Lap-Keller	-0.5 %	12.9 %	27.9 %	32.9 %	14.0 %	23.4 %
Series-60	-1.0 %	11.6 %	37.3 %	42.7 %	15.2 %	23.3 %
Hollenbach	-1.0 %	9.7 %	-0.2 %	11.2 %	3.5 %	13.3 %

Numerical methods

Numerical methods for estimation of wave resistance are further subdivided into:

1. Potential theory
2. Computation Fluid Dynamics (CFD)

Potential theory methods are boundary element methods where the fluid volume around the hull is constrained by boundary conditions. The submerged part of the hull is divided into panels. In potential theory the main assumption is irrotational incompressible inviscid flow. There exist potential flow methods in two dimensions that do not require discretization of the hull shape in a normal manner, i.e. slender ship theory. The motivation for this simplification is that the three-dimensional hydrodynamic problem can be reduced to a set of two dimensional "strips" (Dariusz 2018). This save computational time, but neglect three dimensional effects. Total forces is obtained by integrating cross sectional two-dimensional forces over the ship length. For ships such as tankers this simplification is acceptable, except locally at bow and stern (Dariusz 2018).
CFD includes the earlier Reynolds-averaged Navier-Stokes equation (RANS), where both the wave resistance and viscous resistance is calculated. Another variant of CFD is the Euler-equations which only calculate the wave resistance. CFD methods have a calculation time in the order of magnitude of hours to days, while strip-theory is in the minute to hours range. The computation time is strongly dependent on the computer used. The accuracy in the result is strongly dependent on the mesh size.

Experimental methods

Shipbuilding contracts normally contain strict requirements for speed - power relation of the ship design. Failure to meet these requirements can lead to substantial financial loss for the yard. Thus, traditional ship model testsare widely used. Resistance of ships can be estimated by use of model tests made in tanks. The model hull used is an accurate replica of a scaled model of the ship hull, excluding small

details. During the resistance tests, the model is towed by means of a thin flexible rope. Thus, the resistance (being identical to the force in the towing rope) is measured. In the trials, the model resistance is measured as a function of velocity. After the test a scaling procedure is used to obtain the full-scale ship resistance.

3.2.3 Representation of sea states

Regular waves do not exist at sea. The wave amplitude and period vary over time, and this is referred to as irregular waves. Standard wave spectrums such as Pierson-Moskowites, and JONSWAP wave spectrum characterise irregular sea states. The wave spectrum expresses the distribution of energy for different wave frequencies (Dariusz 2018). These spectra represent the sea states and are suitable for different types of irregular sea i.e. different ocean areas. Pierson-Moskowits spectrum is suitable for fully developed sea, i.e. a sea state where the wind has been blowing long enough over sufficiently open stretch of water, so that the high frequency waves have reached equilibrium (Dariusz 2018). The JONSWAP spectrum is suitable for the North Sea, and do not represent a fully developed sea.

3.3 Ship propulsion

To determine the required power for a given ship design, open water tests and propulsion test can be used.

3.3.1 Open water test

In the open water test the propeller performance with undisturbed inflow is tested. The test is performed without a ship hull present and with the propeller attached in front of the towing equipment, see figure is displayed in Figure 3.3.1.

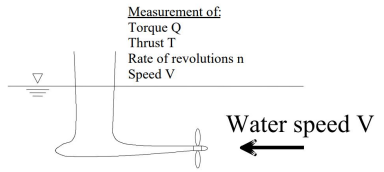

Figure 3.3.1: The picture is taken from compendium in Experimental methods in marine hydrodynamics (Steen 2014*a*)

3.3.2 Self propulsion test

In the self propulsion test the propeller-hull interaction effects are taken into consideration. The test is performed with a scaled hull model fitted with a scaled propulsion system. Together with the results from the open water test it possible to study wake-, thrust deduction effects, and estimate required power as displayed in Figure 3.3.2

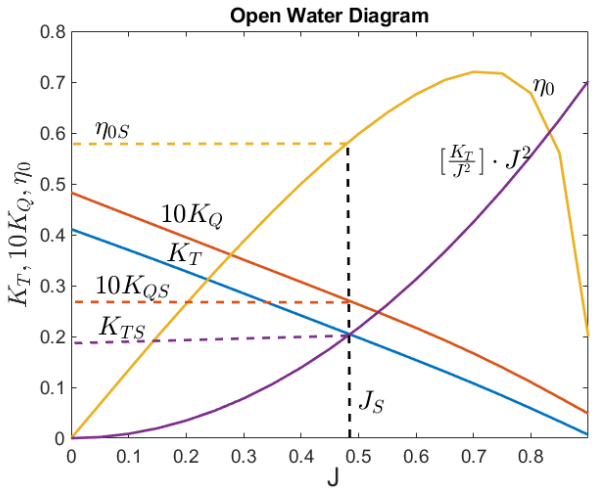

Figure 3.3.2: Open water diagram and propeller working point

3.4 Seakeeping performance

"*Seakeeping performance is the ability of the ship to fulfil its function in environmental conditions which the ship is likely to encounter in its lifetime or over a long-term interval*"(NORFORSK 1987). A merchant ships seakeeping performance is related to its ability to deliver cargo and passengers safely and precisely from origin to destination regardless of sea condition. The function of the ship may be viewed in light of different criterias, such as:

- Short transit time
- Low fuel consumption
- Comfort of passengers and crew in term of accelerations and motions

The effects of seaway and weather reduce the ship performance compared to calm sea performance. Speedloss during a voyage may occur voluntarily or involuntarily. Involuntary speedloss occur due to added resistance caused by wind and waves, and reduced propulsive efficiency and increased propeller loads due to ship motions. Voluntary speedloss is due to captains demands. The captain controls throttle and rudder demands. The main concerns of a captain sailing in a seaway that can result in speed reduction, (NORFORSK 1987), is risk of:

1. Slamming
2. Propeller racing
3. Deck wetness
4. Rolling and lateral motions

5. Excessive vertical motions

3.4.1 Slamming

Slamming occurs when ship bottom hits the water surface at a high velocity. Slamming occurs more frequently on the fore part of the ship and when ship is in ballast condition. Slamming is a larger problem for ships with large block coefficients than for fine ship forms. A captain typically reduce speed if slams occur more than three out of 100 waves (Faltinsen 1990).

3.4.2 Propeller racing

Propeller racing occur when the propeller blades are lifted clear of the water resulting in sudden increase in number of revolutions made by the engine.

3.4.3 Deck wetness

In heavy storm the waves and the ship motions can become so large that water flows on deck of the ship. This phenomenon is called "deck wetness" or "green water".

3.4.4 Rolling and lateral motions

Roll and lateral motion criteria covers the working conditions of ship personnel and safety of cargo.

3.4.5 Vertical motions

Vertical acceleration criteria at forward perpendicular (FP) cover the safety of ship hull and cargo, whilst vertical acceleration at bridge cover crew safety and performance.

Chapter 4

Modelling of ship operation

4.1 General aspects

The computational ship model, hereby referred to as ship model and ship system model, is used to create table look-up datasets by simulating combinations of sea states, wave directions and vessel speed. Available model tests conducted on ship design have been used to build the ship model. Further, the table look-ups is used as input to the discrete-event sea passage simulator, hereby referred to as sea passage model, created by Sandvik et al. (n.d.). In this chapter theory and methods applied to build the ship model and sea passage model is presented.

4.2 Ship system model

Modelling of ship system behaviour is a key success factor of an operational simulation. A ship system is complex and can be computational intensive. It is therefore a compromise between accuracy and simplicity when it comes to operational simulation of a ship system. In this study the focus is on simulating operational decisions in ship design, therefore only information available at the design stage and related theory is relevant.

4.2.1 Ship design

For this study a ship design is used with available towing test for resistance measurements, a propeller open water test and a propulsion test in towing tank. Scaling of the results is done according to the standard correlation method for the model basin where the tests were conducted.

Resistance test

For the resistance test the model is towed by means of a thin flexible rope. The resistance is then equal to the force in the rope. The model is guided, and hence

allow free trimming.

Propulsion test

In this test the model is fitted with a propeller driven by an electrical motor. It is also here toed by the aforementioned rope to compensate for the models increased surface friction, compared to that of the ship. Before the measurements of the torque and thrust in the propeller shaft, the propeller revolutions are adjusted to match the model speed with a pre-selected carriage speed.

4.2.2 Ship motion and added resistance in waves

For calculating added resistance in waves and seakeeping performance ShipX Veres has been used. The theory applied in VERES program is based on linear potential strip theory. The theory is developed for moderate wave heights inducing moderate motions on a ship with length much longer than the ship breadth and draught (Dariusz 2018). Thus, large wave heights and ship motions restricts the validity of the result (Dariusz 2018).

Added resistance in waves

For calculation of short-term added resistance coefficients due to waves, the generalised approach of Gerritsma and Beukelman by Lukakis and Sclavounos, covering oblique waves, is applied. The theory is based on the determination of radiated energy of the damping waves and strip-theory approximation. The Gerritsma and Beukelman method is known to give conservative estimates of the added resistance (Dariusz 2018).

Representation of sea states

At sea the wave amplitude and period wary over time, and this is referred to as irregular waves. An irregular sea state can be characterised by standard wave spectrums such as Pierson-Moskowite, and the JONSWAP wave spectrum (Dariusz 2018). A wave spectrum express the distribution of wave energy for different wave frequencies. A standard spectrum is suitable for different ocean areas. In this study The Pierson-Moskowits spectrum is applied. This spectrum is suitable for fully developed seas. A fully developed sea state refers to "when the wind has been blowing long enough over a sufficiently open stretch of water for high frequency waves to reach equilibrium" (Dariusz 2018).

4.2.3 Operability limiting criteria

Oprability is here referred to as the degree of which a seagoing vessel is able to satisfy specified seakeeping criteria. Theory on the subject can be found in Section 3.4. The limiting criteria are related to safety and comfort of passengers and crew, but also safety and capacity of vessel and operational considerations. Speedloss during a voyage may occur voluntarily or involuntarily. Involuntary speedloss occur due

to added resistance caused by wind and waves, and reduced propulsive efficiency and increased propeller loads due to ship motions. Voluntary speedloss is due to captains demands. The captain can control speed and heading. The operability limiting criteria are used to represent a captain's voluntary speed reduction choice during simulations. NORFORSK (1987) general operability limiting criteria for merchant ships are implemented:

Table 4.2.1: General operability limiting criteria

Criterion	Probability	Limit	Location
Vert.acc.rms	-	0.17g RMS	FP
Vert.acc.rms	-	0.15g RMS	Bridge
Lat.acc.rms	-	0.12g RMS	Bridge
Roll rms	-	6°	Midship
Slamming	2%	-	Bow
Deck wetness	5%	-	Stern-midship-bow
Prop.emergence	0.25%	-	Propeller

4.2.4 Total resistance, propulsion and machinery

The total ship resistance R_T is modelled as:

$$R_T = R_{T0} + R_{AW} \tag{4.2.1}$$

Where R_{T0} is total ship resistance in calm water and R_{AW} is added resistance in waves. Ship resistance in calm water is available from calm water model test, and added resistance is calculated by use of Strip Theory in ShipX Veres, see section section 4.2.1 and section 4.2.2. Wind resistance and roughness resistance is not considered in this study. The propulsion of the ship is modelled by use of open water diagram for full-scale propeller where thrust identity is considered. For this purpose model data for resistance (resistance model test), propeller characteristics (open water model test) and propulsion (self-propulsion test) are available. The propulsion of the ship is modelled according to the standard correlation method given for the specific model basin. The following procedure can be found in Steen (2014*b*) and Brockhaus (2011). For the open water diagram propeller advanced velocity J, propeller thrust T, and torque Q are represented in dimensionless form as:

$$J = \frac{V_A}{nD} \tag{4.2.2}$$

$$K_T = \frac{T}{\rho n^2 D^4} \tag{4.2.3}$$

$$K_Q = \frac{Q}{\rho n^2 D^5} \tag{4.2.4}$$

where ρ is the water density, n the propeller rate of revolutions, D the propeller diameter and V_A the advance speed of the propeller. The working point of the

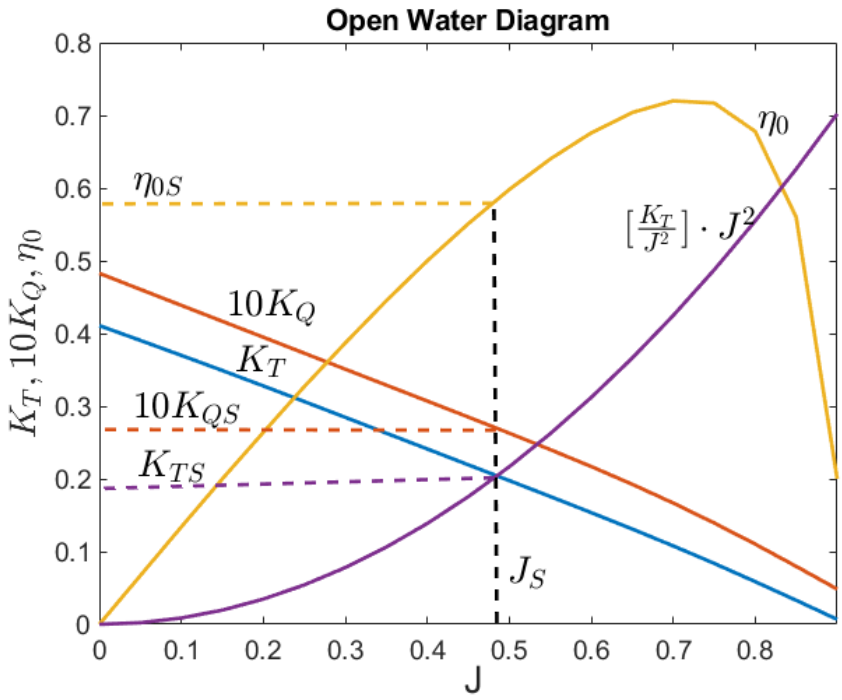

Figure 4.2.1: Open water diagram and propeller working point

propeller is defined as:

$$\frac{K_T}{J^2} = \frac{R_T}{(1-t)(1-\omega)^2 V_s^2 D^2 \rho} \tag{4.2.5}$$

t is the thrust deduction factor from a thrust variation test, ω is the effective wake fraction of the ship from the full-scale corrections of the effective wake fraction of the model. An example of such a diagram can be found in Figure 4.2.1. A detailed description if the involved model test procedures and definitions can be found in Steen (2014*b*), and will not be described here.

When multiplying the range of J^2 by equation eq. (4.2.5), a curve for the required thrust is obtained. The intersection of the curve with the thrust coefficient curve, K_T gives the propeller working point. An example can be found in Figure 4.2.1. For this working point, the required propeller torque coefficient $10K_{QS}$, the open water efficiency η_{0S} and advance ratio J_S are obtained. Assuming thrust identity and available open water and propulsion tests, the relative rotative efficiency η_R is known. Then the propeller rate of revolutions,

$$n = \frac{V_s(1-w)}{J_S D_S} \tag{4.2.6}$$

the delivered power,

$$P_D = 2\pi\rho n^3 D^5 \frac{K_{QSB}}{\eta_R} \tag{4.2.7}$$

and the engine brake power, given a mechanical efficiency η_M,

$$P_B = \frac{P_D}{\eta_M} \tag{4.2.8}$$

are obtained and can be used as input for the engine operation diagram. Further, the specific fuel oil consumption is given by engine shop test curve.

4.3 Sea Passage Model

The sea passage model is created as part of SFI Smart maritime research and presented in Sandvik et al. (n.d.). An illustration of the procedure is reproduced in Figure 4.3.1

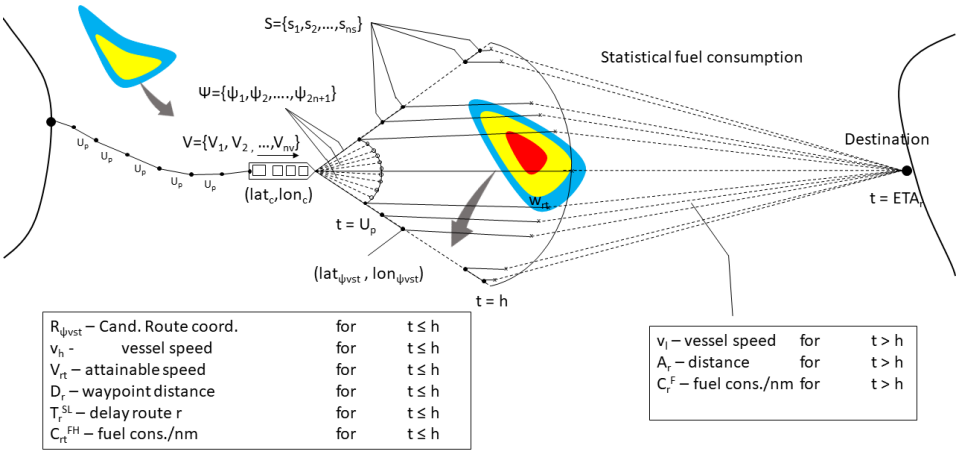

Figure 4.3.1: Sea passage model by Sandvik et al. (n.d.). Overview with variables and parameters

4.3.1 Route generation

The great circle route from current location to destination is used as a basis for route generation. To each side of the shortest route, n candidate headings are created based on a set maximum offset angle ψ_{max}. From these initial headings, candidate routes are divided in ns segments of equal distance and spanned h hours into the future. For each segment, a great circle route is generated toward the destination. For $t \geq h$ a statistical model is used, see section section 4.4.1.

4.3.2 Weather update

It is assumed that reliable weather forecast is available for h hours into the future. Beyond this the weather is considered unknown. The simulator updates route and speed with intervals of u_p hours. In this update the weather h hours into the future are considered. Wave hindcast data-sets are used to replicate the conditions encountered along a route. The data is stored in a table look-up matrix indexed by latitude, longitude and time. A table for significant wave height (Hs), spectral peak period(Tp) and wave propagation direction(α) are available. Spatial and temporal interpolation is used to estimate Hs, Tp and α for a way point in the simulation. NaN values are found for areas with landmass. Routes crossing such areas are discarded in the simulation.

4.3.3 Fuel consumption and delay estimation

The fuel consumption rate and required power in each route leg at time $t \leq h$, in sea state W_{rt} with vessel speed V_{rt} is estimated base on a table look-up model. Pre-generated matrices indexed by Hs, Tp, V and α for power- and specific fuel oil consumption are predicted based on theory presented in Section 4.2.4. If v_h requires more power then installed power, or operability limiting criteria is exceeded, v_{rt} is reduced accordingly. At $t = h$ a great circle route to the destination with distance A_r is calculated. Fuel consumption for distance A_r is based on a statistical model, section 4.4.1. The estimated time of arrival ETA_r is calculated base on Equation (4.4.2). If v_{rt} contains reduction the delay period T_r^{SL} increases accordingly.

4.4 Optimization procedure

The sea passage behaviour is controlled by target speed and delay cost. At simulation initiation a target time of arrival T_0 is calculated based on the great circle route from origin to destination, with the set target speed. The sea passage model attempts to complete the voyage using a minimum amount of fuel and delay cost. The objective function is a mathematical formulation of the decision making processes for speed and heading during sailing. The objective here is to minimize fuel consumption and delay cost,

$$min \sum_{r \epsilon R_{\psi v_h v_l s}} \sum_{t \leq h} \Big(C_{rt}^{FH} D_r + C_r^F A_r + \kappa \tau_r \Big) x_r \tag{4.4.1}$$

The distance covered on time interval $t \leq h$ is given by route, speed v_h and sea state W_{rt}, for which the fuel cost rate C_{rt}^{FH} and delay due to speed loss T_r^{SL} is calculated. D_r is the waypoint distance, A_r is the distance from end of observable horizon to destination and C_r^F is the statistical fuel consumption. κ is a linearly increasing delay cost rate, and τ_r is the estimated delay time. x_r is a binary variable that is equal to 1 if speed v_h is chosen for the fist h hours, Speed v_l is chosen for the

remaining part of the voyage, heading ψ and route extension interval S is chosen, 0 otherwise.
The estimated delay time is calculated by:

$$\tau_r = t_c + h + \frac{A_r}{v_l} + T_r^{SL} - T_0 \tag{4.4.2}$$

where t_c is the current simulation time. To model a dynamical speed planning strategy, a speed profile for the observable horizon is formulated. During the observable horizon the vessel can obtain three differed speed levels, v_1^{ga}, v_2^{ga} and v_3^{ga} at time t_1^{ga} and t_2^{ga}, see Figure 4.4.1. To select the optimal speed profile a genetic algorithm heuristic in MATLAB is used to evaluates the objective function in Equation (4.4.1).

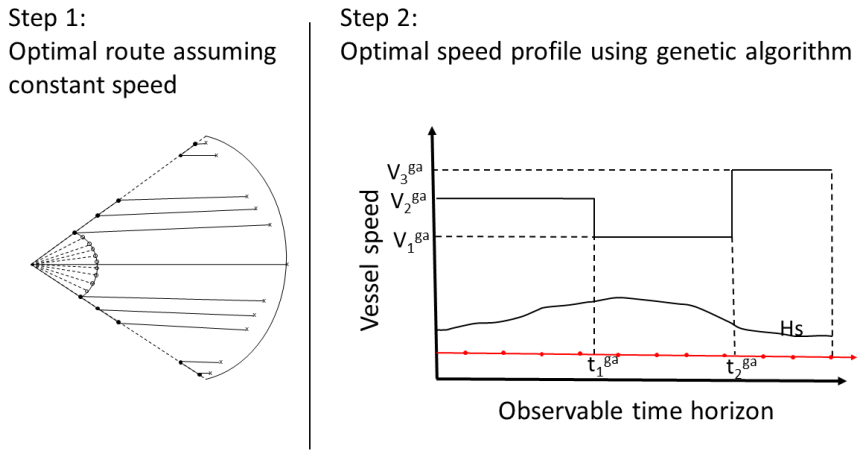

Figure 4.4.1: Optimization procedure divided in two steps for providing heading and speed intput for sea passage model. From Sandvik et al. (n.d.).

4.4.1 Statistical Sea Passage Model

To estimate the fuel- and delay cost for the remaining part of the voyage $t \geq h$, a long term statistical approach has been applied. In this model only head waves are assumed.

Long term wave statistics

While short term statistics are calculated for a certain sea state where the significant wave height and peak period are assumed constant, long term wave statistics provide predictions when the time period is longer than the duration of one sea

state, i.e. the significant wave height and peak period varies. Thus, the probability of occurrence of the sea states are required. The joint probability of significant wave heights and characteristic period is often presented in a wave scatter diagram. As for wave spectra in short term statistics, wave scatter diagram in long term statistics are also suitable for certain ocean areas. The conditional modelling approach (CMA) recommended by DNV GL (2017) is applied in this study. The significant wave height is modelled by a 3-parameter Weibull probability density function and given by:

$$f_{H_s}(h) = \frac{\beta_{H_s}}{\alpha_{H_s}} \left(\frac{h - \gamma_{H_s}}{\alpha_{H_s}} \right)^{\beta_{H_s}-1} \exp\left(- \left(\frac{h - \gamma_{H_s}}{\alpha_{H_s}} \right)^{\beta_{H_s}} \right) \tag{4.4.3}$$

A log normal distribution is used for the zero-crossing wave period, given a Hs:

$$f_{T_z|H_s}(t|h) = \frac{1}{\sigma t \sqrt{2\pi}} \exp\left(- \frac{(\ln t - \mu)^2}{2\sigma^2} \right) \tag{4.4.4}$$

μ and σ are functions of the significant wave height and modelled as:

$$\mu = E[\ln T_z] = a_0 + a_1 h^{a_2} \tag{4.4.5}$$

$$\sigma = std[\ln T_z] = b_0 + b_1 e^{b_2 h} \tag{4.4.6}$$

Distribution parameters for world wide operation of ships is used as found in table C-5 DNV GL (2017), and valid for the following world wide sailing routes: Europe - USA East coast, USA West coast - Japan - Persian Gould - Europe (around Africa).

Table 4.4.1: Distribution parameters for average world wide operation of ships found in Table C-5 page 246 (DNV GL 2017).

α_{H_s}	β_{H_s}	γ_{H_s}
1.798	1.214	0.856
a_o	a_1	a_2
-1.010	2.847	0.075
b_0	b_1	b_2
0.161	0.146	-0.683

The occurrence probability $p(h_s, t_p)$ for a set of sea states (h_s, t_p) $\epsilon\Gamma$ is given by:

$$p(h_s, t_p) = f_{H_s} \cdot f_{Tp|H_s} \tag{4.4.7}$$

since a continuous distribution have been discretized, $p(h_s, t_p)$ is divided by the sum of all probabilities, to make sure that they sum to 1.

Attainable speed

Further, the available average speed $\overline{V}_{att}(hs, tp)$ based on attainable speed V_{att} is required and given by:

$$V_{att}(h_s, t_p) = \min(V_{req}, V_{att}^{isl}(h_s, t_p), V_{att}^{vsr}(h_s, t_p)) \tag{4.4.8}$$

where V_{req} is the requested speed, $V_{att}^{isl}(h_s, t_p)$ is the attained speed due to involuntary speed loss in sea state $(h_s, t_p)\epsilon\Gamma$ due to V_{req} requres more power than installed, see Section 4.2.3. $V_{att}^{vsr}(h_s, t_p)$ is the voluntary speed reduction due to ship handling concerns described in section 4.2.3. The expected average attained speed $\overline{V}_{att}$ is then given by:

$$\overline{V}_{att}(V_{req}) = \sum_{(h_s,t_p)\epsilon\Gamma} p(h_s, t_p) \cdot V_{att}(h_s, t_p) \tag{4.4.9}$$

Statistical fuel consumption

The weighted average fuel consumption based on the table look-up fuel consumption can be found by:

$$\overline{f}_c(V_{req}) = \sum_{(h_s,t_p)\epsilon\Gamma} p(h_s, t_p) f_c(h_s, t_p, V_{att}) \tag{4.4.10}$$

For the remaining sailing distance $t \geq h$ the ship sails with constant speed and follows the great circle route.

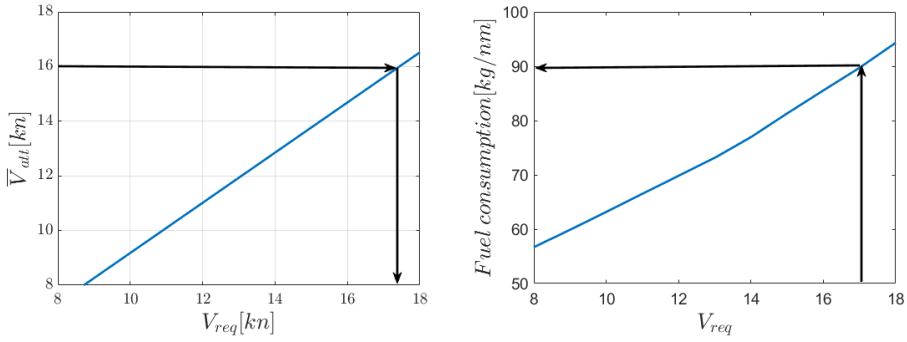

(a) (b)

Figure 4.4.2: Statistical average speed and fuel consumption model

Speed loss

Voluntary speed loss is modelled using the operability limiting criteria for merchant ships presented in *Assessment of ship performance in a seaway* (NORFORSK 1987). It is calculated by use of ShipX operability analysis (short-term statistics in the frequency domain) (Dariusz 2018). The maximum power output for the engine

is set to be 100 % maximum continuous rating (MCR). The simulation is set to accept speed loss if required power exceeds this level. When the ship is faced with extreme weather it will in some circumstances not be able to maintain any speed. To avoid infinity values in fuel consumption involuntary speed loss V_{ivsl} is set to 1 knot under such circumstances.

4.5 Wave attack angle definition

In this thesis the definition for wave attack angle displayed in Figure 4.5.1 is used.

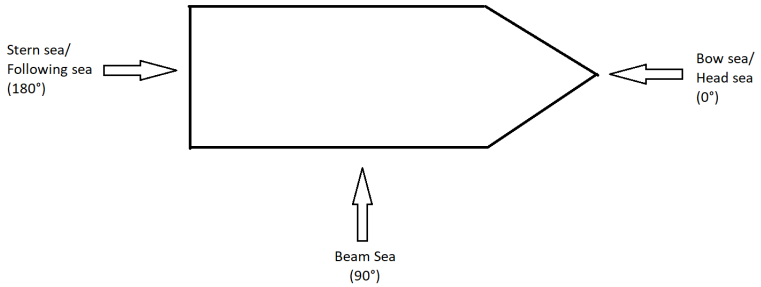

Figure 4.5.1: Wave attack angle definition

Chapter 5

Case vessel

The case vessel is a general cargo carrier outfitted with a real-time performance monitoring system. The particulars for the case vessel is given in Table 5.0.1. The vessel is a single screw vessel outfitted with a Mewis duct and has a single main engine.

Table 5.0.1: Case vessel particulars

Length [m]	Beam [m]	Design draught [m]	Gross tons [Tons]	Design speed [kn]
204	32.3	12.5	37 000	15.5

5.1 Data acquisition

The data is provided is from the period of 2014 to 2017. The data is recorded as time series, with 15 minutes intervals. A list of applied parameters are given in table 5.1.1

Table 5.1.1: Data acquisition parameters and measuring techniques

Parameter	Measuring technique
Shaft toque, RPM and power	Optical sensors
Fuel consumption	Fuel line flowmeter
Speed through water	Doppler sonar
Speed over ground	GPS
Position	GPS
Wind	Anemometer

Chapter 6

Model verification and validation

As a means to increase the utility value of the research a validation and verification study of the ship model is conducted. The decision-making process of the sea passage model relies on the ability to forecast ship behaviour. Definitions and techniques from Section 2.3 is used. Firstly, a conceptual model validation is presented for the ship model followed by a validation of the data set used. Finally, a historical data validation of the ship model is presented and compared to full-scale data.

6.1 Conceptual model validation

Conceptual model validation is done to determine correctness of theories and assumptions underlying the conceptual model and validate if the model representation of the problem entity is "reasonable" for the intended purpose of the model. To address this topic the uncertainty and error in relation to the underlying theories and assumptions for the conceptual model is addressed. Each step in the simulation, i.e. from applied weather to power prediction, is a potential source of error. The errors are caused by physical phenomenon not described by the model and assumptions in applied theory. Models that are not able to capture and sufficiently describe the system state and underlying factors will cause errors. This section provides an overview of the most prominent and detected sources of error and their influence.

6.1.1 Hydrodynamics

To replicate vessel performance in a sea way presents great modelling challenges. For fuel consumption the main concerns are related to resistance and propulsion efficiency.

Resistance

Ship resistance calculation is a complex task due to the fact it does not originate from one source, but many. The calm water resistance to speed relation was initially based on calm water model tests and corrected through comparison with full-scale measurement for the ship design. Definitions for wave attack angles can be found in Figure 4.5.1. For following seas and stern quartering seas the added resistance are mostly estimated to give a negative contribution to the total resistance, see Figure 6.1.1. To avoid large negative contributions that are unrealistic for the simulator all negative contributions are set to 0. For significant wave height of 1 meter and vessel speed of 14 knots the added resistance is maximum 4 % of the calm water resistance whereas for wave height of 10 meters it can be up to 400 % of the calm water resistance contribution. Also for low vessel speeds and high sea states, fig. 6.1.2, the added resistance contribution becomes dominant.

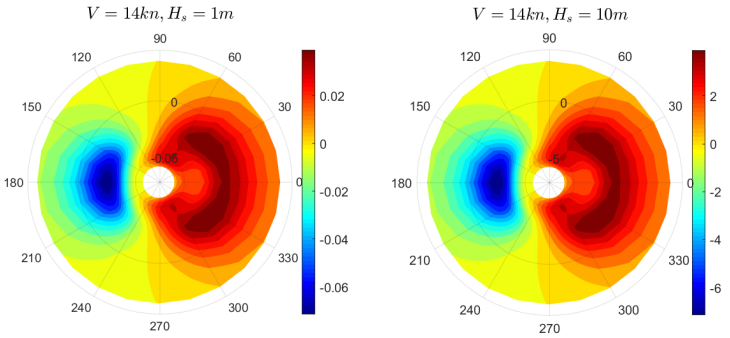

Figure 6.1.1: Added resistance faction of calm water resistance for wave attack angle of 0 to 360 degrees and vessel speed 14 knots

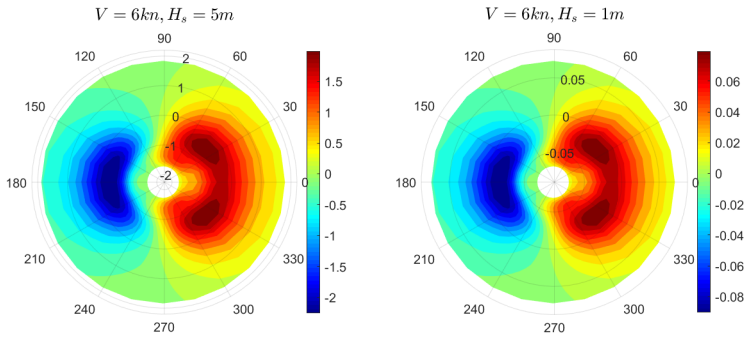

Figure 6.1.2: Added resistance faction of calm water resistance for wave attack angle of 0 to 360 degrees and vessel speed 6 knots

Draught influences the underwater hull surface area and hull form. The draught varies during the course of a voyage, weather and loading conditions. For this simulation the draught is held constant and is therefore a source of error.

6.1.2 Operability limiting criteria

Due to the propeller positioning not being known with certainty, a sensitivity analysis with propeller position used in the model test as basis is conducted in relation to operability limiting criteria, section 4.2.3. The analysis has been conducted for a selection of speed and heading combinations. In Figure 6.1.3 we see the difference between lowest and highest propeller positioning gives a difference of about 1 meter in significant wave height. The propeller emergence criterion is found to be the limiting criterion for close to all sea states. All calculations are done for draught of 10.5 meters, which is 2 meters below design draught. This was done to make the model conditions similar to what was experience by the comparison vessel for the voyages that were selected. This is a contributing factor to propeller emergence being the limiting criterion.

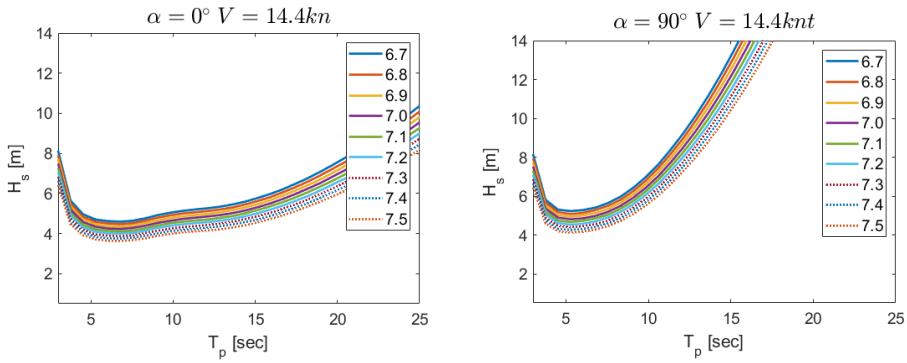

Figure 6.1.3: Operability limit for varying propeller positions conducted in ShipX VERES in meters above the keel

Manoeuvring

Manoeuvring causes an increase of resistance due to rudder drag and hull angle of attack relative to the direction of travel (Sandvik et al. 2018). The hydrodynamic model applied in this simulation does not account for these effects. It strictly simulates only the sea passage, disregarding the periods where the vessel is in manoeuvring mode close to port. Land or shallow sea may require our vessel to manoeuvre around. This is accounted for by excluding routes where wave data is not available from candidate route selection in the sea passage model.

6.1.3 Weather data

The hind cast database relies on state-of-the-art meteorological services. A six-hour time resolution is used for the simulation. If conditions are rapidly changing in time and space. This will not be captured accurately in our simulation. There exists uncertainty due to grid size in data. Time and space interpolations are conducted when retrieving weather data.

6.1.4 Vessel and machinery condition

Vessel and machinery conditions affect the vessel performance. Increased roughness on hull due to marine growth, fouling, corrosion etc. can cause a significant increase in required power. Propeller fouling causes reduced efficiency. Machinery maintenance affects fuel consumption and the combustion process. To correct for ideal circumstances during shop test and propulsion test a correction in the specific fuel oil consumption curve is conducted in section 6.3.2.

6.1.5 Quasi-static estimation

Quasi-static estimation of added resistance due to waves assumes a characteristic steady-state to be valid for the duration of the sea state. Sailing is in reality a dynamic process with transient loading in varying sea states.

6.2 Data validity

There has not been conducted an independent validation of the given data. However, a study of accuracy and validity of such systems have been reviewed. Hasselaar (2011) have investigated the feasibility of the real-time ship performance monitoring and analysis (PM&A) system for collection of full-scale measurements. A system evaluation was conducted on a small research vessel (16 meters) and a large vessel (300.000 dwt crude oil tanker). The viability of the proposed algorithms and design principles for PM&A system was proven successfully. Scatter in long term key performance indicators (KPIs) was reduced to ± 12 %. It is pointed out that automatic logging of wave characteristics could increase accuracy. Information about encountered waves could have increased accuracy for the correction of calm water resistance curve as well.

6.3 Historical validation of ship model

Historical full-scale data for ship operations have been used for model validation. Towing test for calm water resistance, open water characteristics, propulsion tests and a shop test for the installed machinery is used to build the ship model. To correct for ideal circumstances during tests, fouling and other defects that have occurred during use, the calm water resistance curve and specific fuel oil consumption curve was tuned to full-scale data for calm seas.

6.3.1 Calm Water Resistance Correction

Initially the model's calm water resistance was based on the calm water model test for the comparison ship. Change in resistance can be caused by fouling and incorrect draught among other things. When comparing model estimates to full-scale data for calm seas, the model displayed a large variation in power for small variations in speed compared to full-scale data. A study of all parameters revealed calm water resistance influencing the variations to a large degree. To tune the calm water resistance curve the following was done:

1. Select data points with low relative wind speeds in a calm period, i.e. June-August
2. Plot power versus speed for full-scale data for the selected data points and find suitable curve fit, see Figure 6.3.1a
3. Establish the calm water resistance curve that gives the power curve found in 2
4. Compare to initial model, see Figure 6.3.1b

The initial model had a much steeper calm water resistance curve compared to an established full-scale resistance curve, making it more sensitive to change in speed, and hence some of the cause for large variations in power compared to full-scale data.

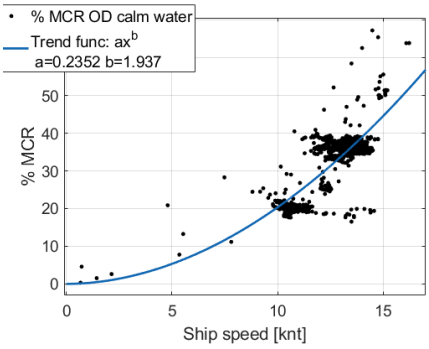

(a) Curve fit for calm water power of full-scale data

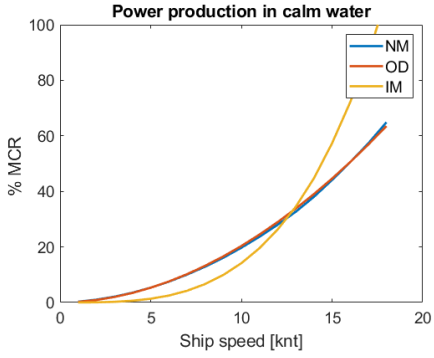

(b) Comparison of power curves. The initial model(IM), the full-scale operational data(OD) and the new model(NM)

Figure 6.3.1

The corresponding equation for the new calm water resistance curve is

$$r_{T0} = 25000 \cdot V_s^{1.116}[N] \tag{6.3.1}$$

After the correction the model display "calmer" tendencies in accordance with the model. In Figure 6.3.2a and Figure 6.3.2b a scatter of how the initial and new

model estimate power compared to full-scale data is displayed. We see that the points are centred more inside the blue area for the new model whereas the initial model stretch above.

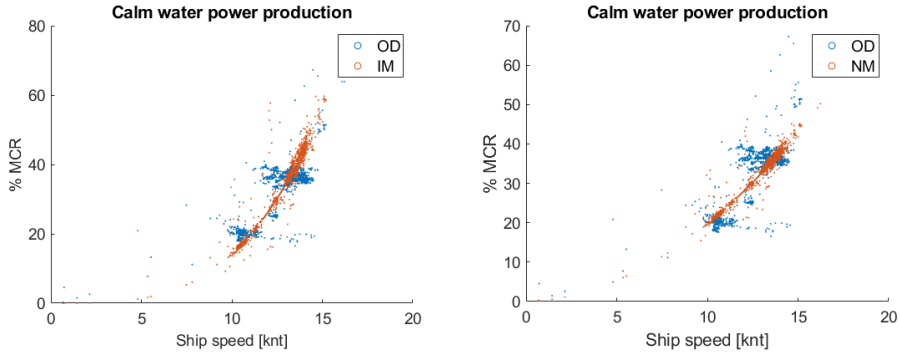

(a) Initial model versus full-scale data (b) New model versus full scale data

Figure 6.3.2

6.3.2 Fuel consumption correction

Increased fuel consumption compared to a shop test can be caused by high temperatures, lack of oxygen and/or deteriorating parts among other things. To correct for this, the same data points as in Section 6.3.1 has been used to create a scatter diagram for added specific fuel consumption, see Figure 6.3.3. The following has been done in the correction process

1. Since specific fuel oil consumption (sfoc) is not given in the dataset, it had to be calculated. The sfoc for full-scale data is found by use of the following equation

$$sfoc = \frac{f_c \cdot V_s}{D \cdot P_B} \left[\frac{kg}{kWh} \right] \tag{6.3.2}$$

   where f_c is fuel consumption in kg, V_s is ship speed in knots, D is distance travelled and P_B is engine break power. This data is displayed as scatter in Figure 6.3.3, marked as OD.

2. A trend-line based on the calculations are created, marked as NM (New model) in Figure 6.3.3.

3. The trend-line is compared to initial sfoc (IM) based on shop test for machinery.

In Figure 6.3.3 we see that the full-scale data contains significant scatter. However, all measured points are above the initial sfoc curve. The new sfoc curve (NM) in Figure 6.3.3 represents an increase of about 25 % compared to the initial curve.

Power production is an exponential function of vessel speed, among other factors. Consequently, small variations in ship speed are magnified into larger variations in power and therefore also fuel consumption.

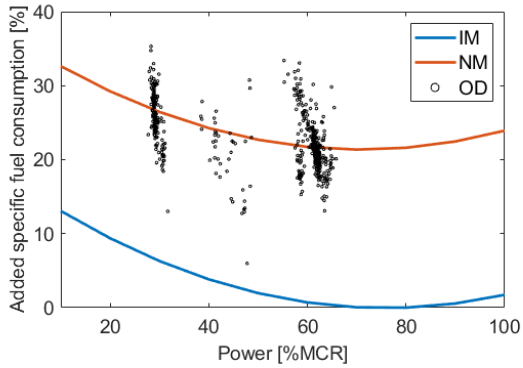

Figure 6.3.3: Added specific fuel consumption for initial model(IM) based on shop test, full-scale data(OD) and the new model proposal(NM) normalised using shop test curve minima

6.3.3 Model VS full-scale data

To see how the model performs compared to full-scale data, a comparison of selected routes is conducted. Location, speed and time from full-scale data is given as input to the ship model. The model uses hindcast wave data for the area collected from *European Centre for Medium-Range Weather Forecast* (2018) and speed to estimate % MCR and fuel consumption. The corrected model displays similar behaviour as full-scale data for wave attack angles below 50 degrees, see Figure 6.3.4a and Table 6.3.1. In Section 6.1.1 it has been shown that the added resistance decrease from bow-quartering sea, and that it has no contribution from beam-seas to stern-seas. As a consequence, total resistance will generally decrease for bow-quartering seas, and result in underestimation of power. This phenomena can be view from waypoint 200 to 1000 in Figure 6.3.4a. In the lowest graph in Figure 6.3.4a % diff in fuel consumption is given in relation of full-scale measurements.
The fuel consumption curve was increased by approximately 25 %, section 6.3.2, but still differs with an average of -7.2 % for wave attack angles below 50 degrees when sailing from Shanghai to Panama. More details from this case study can be found in Appendix A.

Table 6.3.2: Full-scale data compared to fixed calculations with ship model

Case	Distance [nm]	Duration [h]	Average speed [kn]	mean %MCR [%]	std [%]	Fuel consumption [ton]	Fuel con. rate [ton/day]	mean Hs [m]
OD	6131	420	14,6	78,5	1,7	519	30	2,7
Fixed	6131	420	14,6	49,9	8,6	485	28	2,7

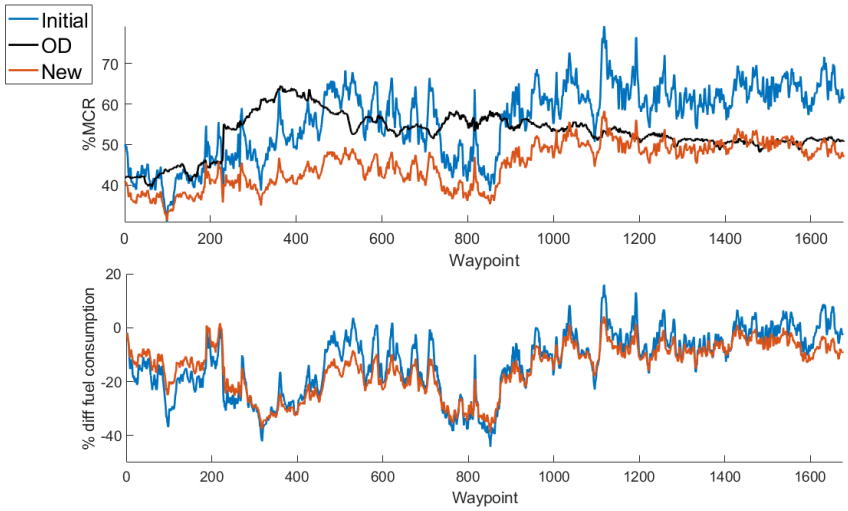

(a) % diff in fuel consumption is relative to full-scale measurements. Initial model is based on a calm water resistance curve from calm water model test. OD is the full-scale measurements. New is the model corrected for full-scale measurements.

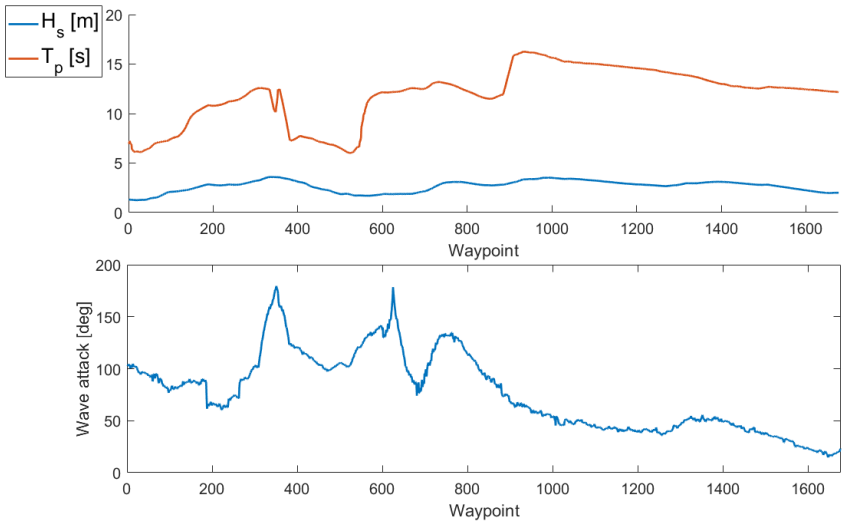

(b) The encountered weather during fixed sailing based on coordinates from full-scale measurements. Wave attack angle are defined as: 0° for head seas and 180° for following seas.

Figure 6.3.4: Operational calculations for initial and new model compared with full-scale data(OD)

Table 6.3.1: Mean and standard deviation of propulsion power and fuel consumption for fixed route comparison with alpha below 100 degrees

Route		Initial model			Corrected model		
		mean diff. power	std	mean diff f_c	mean diff. power	std	mean diff f_c
To	From	[%MCR]		[%MCR]	[%]		[%]
Shanghai	Seattle	14,1	± 6,0	-0,6	-5,2	± 4,5	-10,9
Shanghai	Panama	11,5	± 4,2	-3,6	-1,7	± 2,3	-7,2

6.3.4 Route selection

On the basis of the established weakness for stern-seas, potential routes were studied and evaluated based on wave attack angle. In order to simulate a route, the weather data for the given time and area had to be available. For the weather data available, three routes from the full-scale measurements were evaluated. Out of the three options, Shanghai Panama and Shanghai Seattle had the least follow sea during voyage and was therefore selected as case routes.

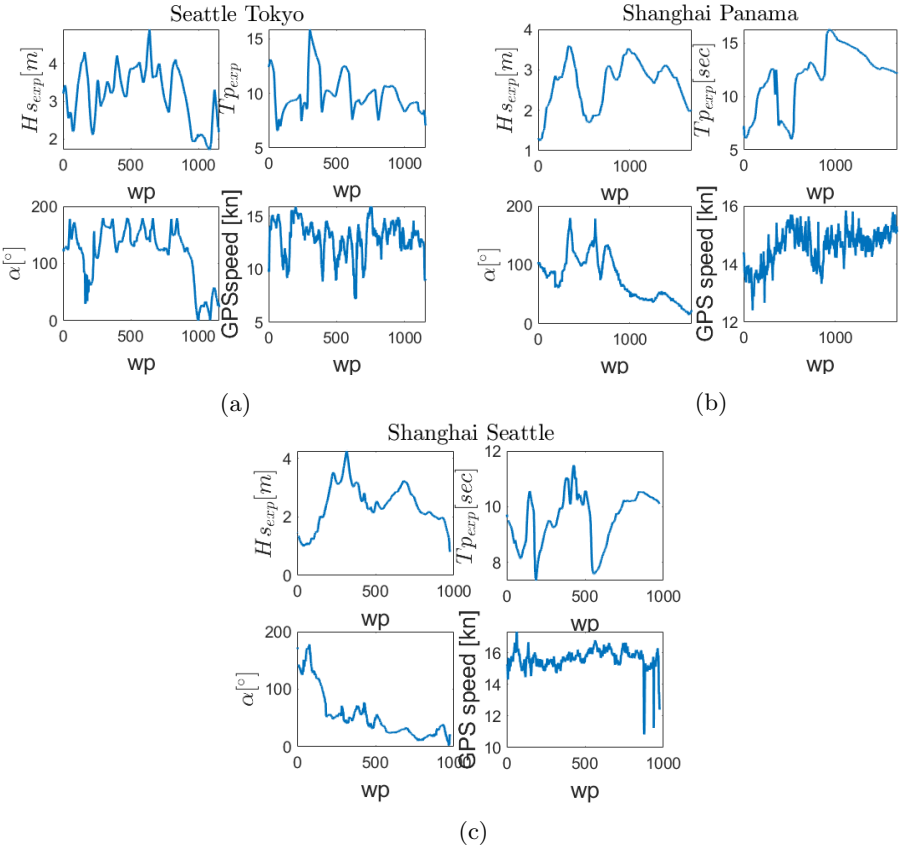

Figure 6.3.5: Weather on alternative routes in full-scale data

Chapter 7

Case description

The primary objective of this thesis is to develop more realistic and accurate simulations of sea passage voyages for application in simulation-based design of ships. By comparing simulations to reality, it is believed it can give a better insight to strengths and weaknesses of both ship model and sea passage model. Hence, the simulated ship operation is compared to full-scale data from an existing vessel. A comprehensive case study has been performed to investigate route and schedule disruption behaviour in simulated ship operation. In this chapter the case study particulars and assumptions are stated. Firstly, the work process is described followed by sea passage model parameters and scenarios. Finally, delay cost models and statistical cost function models is given for each scenario.

7.1 Work process

A ship model is proposed in Section 4.2 and validated by use of full-scale data in Chapter 6. A selection of routes for the case study is presented and selected based on the model validity for the specific route in Section 6.3.4. An initial study was conducted on route 1; Shanghai Panama in order to familiarize with the sea passage generator and compare simulations to full-scale data. For this study the same sea passage model parameters as in Sandvik et al. (n.d.) was applied with linearly increasing delay cost rate κ selected as described in Section 8.3.2. From this study two main questions aroused:

- How does length of horizon affect simulations? (Sec.8.2)
- How does delay cost affect simulations? (Sec.8.3)

Weather forecasts are subject to uncertainty, and generally a function of lead time between forecast issuance and time of realisation. This uncertainty is neglected in the model. Hindcast data is used as forecast, thus ensuring the model is able to make the best decision possible within the observed horizon. In the model an abrupt end to available information at the end of the horizon is assumed. A ship

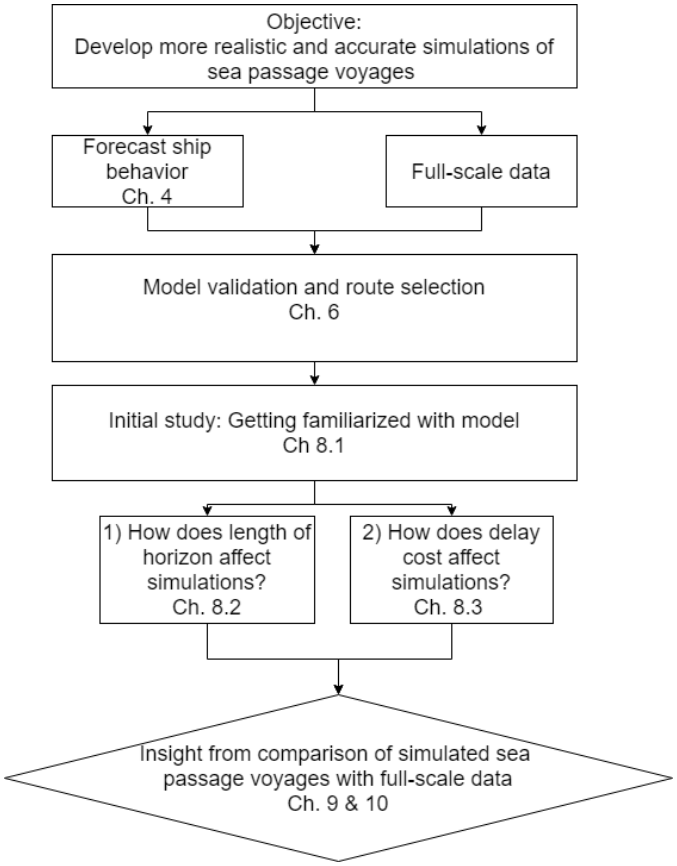

Figure 7.1.1: Work process

sailing in reality is subject to this uncertainty and will not have an abrupt end to available information but process the increasing uncertainty. To investigate the impact of horizon length on a route selection a sensitivity study for horizon lengths is conducted, see Section 8.2. The horizon length is varied from 48 hours to 120 hours and compared to full-scale data.

The basis on which decisions are made in the sea passage model is stated in the objective function. Two main considerations are made. Firstly, it attempts to complete the voyage using a minimum amount of fuel. Secondly, it is motivated to complete the voyage within target time by the cost function. To get a better understanding of how target time and delay cost affects the simulations, a study of target speed and linear delay cost with rate κ influence on route selection and operational parameters were conducted and presented in Section 8.3.1.

Further, an attempt of creating general cost functions forms was made and imple-

mented in the sea passage model, representing agreements between ship owner and cargo owner as well as ship owner and captain. Five different functions were tested and is described in section 7.4.2. The results are presented in Section 8.3.2

7.2 Sea passage model parameters

Vessel speed is assumed to vary on an interval between 11 and 18 knots with a spacing of 1 knot. This level of discritization is chosen to reduce the number of options to evaluate in the sea passage model, thus decrease computational efforts. A maximum offset angle of ψ_{max} relative to the current location and destination following the great circle route is used in route generation. Spacing between headings n and route segments n_s is set to n=n_s=10, as recommended after the convergence study conducted by Sandvik et al. (n.d.), and will therefore not be subject of further study here. At simulation initiation the target time is set based on distance of the great circle route and target speed. Arrival at time t ≥ target time will introduce delay costs. The optimization routine is initiated every u_p hours and provides new heading and speed commands.

Table 7.2.1: Sea passage model parameters

Parameter	V [kn]	ψ_{max} [deg.]	n=n_s [-]	u_p [h]
Value	11:1:18	±45	10	6

7.3 Routes

Two voyages over the North Pacific is simulated and compared to full-scale data. Hindcast wave data is collected from *European Centre for Medium-Range Weather Forecast* (2018). Simulation are terminated when distance to destination is lower than $u_p \cdot V_{max}$. Only the transit part of the voyages is simulated. Hence, first and last part of voyages is removed.

Table 7.3.1: Route specifications

From	Coordinate	To	Coordinate	Dits. g.c [nm]	Month	Mean draught fore [m]	Mean draught aft [m]
Shanghai	30°44'N 133°39'E	Panama	21°03'N 111°38'W	6211	January	8.4	9.3
Shanghai	41°41'N 142°57'E	Seattle	48°32'N, 133°34'W	3554	September	8.1	8.8

7.4 Scenarios

Scenarios are generated through different combinations of target speed, V_t, horizon length, hor, linearly increasing delay cost with rate κ and delay cost function form, y_n. An overview of all simulated combinations is found in Table 7.4.1.

Table 7.4.1: Scenario overview

Section	Description	Route		Constants	Variables
8.1	Initial Case	Shanghai	Panama	V_t=15.4 kn, hor=72 h	κ=1.2:0.2:1.6
8.2	Length of Horizon	Shanghai	Panama	V_t=15.4 kn, κ=1.2	hor=48:24:120 h
8.2	Length of Horizon	Shanghai	Panama	V_t=15.4 kn, κ=1.2	hor=102:6:114 h
8.2.2	Length of Horizon	Shanghai	Seattle	V_t=15.7 kn, κ=1.4	hor=48:24:120 h
8.3.1	Target time and linear κ	Shanghai	Panama	[-]	V_t=[14.1 15.4 16.4] kn, κ=1:0.2:2.6, hor=[72 120] h
8.3.1	Target time and linear κ	Shanghai	Seattle	[-]	V_t=[13.8 14.8 15.7] kn, κ=1.2:0.2:1.6
8.3.2	Cost Function Form	Shanghai	Panama	V_t=14.1 kn, Cost func.=[y_0 y_1 y_2 y_3 y_4]	hor=[96 120] h

7.4.1 Target speed

The selected target speed is based on the arrival time at destination for comparison vessel and the statistical cost function model, see table 7.4.2.

Table 7.4.2: Target speed and time for arrival for scenarios

Route	V_t	Description	Target time of arrival
Shanghai Panama	14.1 kn	Based on distance traveled divided by time for comparison vessel	420 h
	15.4 kn	The statistical required speed to obtain an average speed of 14.1 kn	385 h
	16.4 kn	A further increase in target speed	361 h
Shanghai Seattle	13.8 kn	Based on distance traveled divided by time for comparison vessel	245 h
	14.8 kn	A further increase in target speed	228 h
	15.7 kn	Average speed of comparison vessel	215 h

7.4.2 Delay cost

The statistical cost model is used as basis for selection of κ and time of arrival for the OD. In Figure 7.4.1a the statistical cost model for V_t=15.4 kn and linear delay cost with rate κ is displayed. κ is given in fuel consumption equivalence. If arriving on or before target time the objective value will only consist of fuel cost. The lowest possible cost is found to be precisely on target time. If the vessel arrives after target time, the delay cost will start adding to the objective value as displayed by solid curves. If rate of κ is set in such a way that the lowest point on the curve is past target time, the sea passage model will find it rewarding to arrive late. If it is set so that it is flat, the vessel has a "slack" on witch time to arrive.

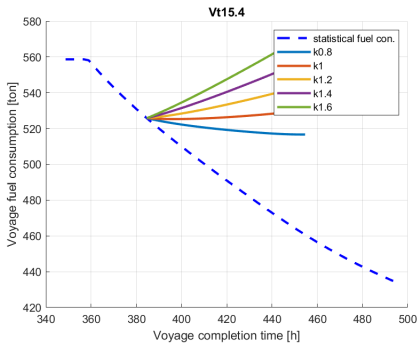

(a) Linear delay cost with rate κ for V_t=15.4 kn

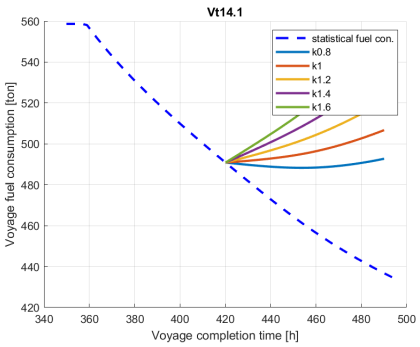

(b) Linear delay cost with rate κ for V_t=14.1 kn

Figure 7.4.1

Function form

In Figure 7.4.2a the delay cost in tons is displayed in relation to delay time τ_r in hours. To compare cost function form and slope values, the statistical cost function model have been used, Figure 7.4.2b. Function y_0 and y_1 represent a linear increasing cost function. For y_0 the delay cost start when the ship arrives delayed, while y_1 rewards early arrivals of up to 10 hours in this case. y_2 represents a contractual day-rate fee for delays. y_3 and y_4 represents a steeper increase in the delay cost. In addition, y_4 has a diminishing delay cost after a certain time and y_3 reward early arrival up to 10 hours in this case. For the functions that rewards early arrival, half the expenses of arriving maximum early contra arriving on time is given as reward for early arrival, i.e. arriving in the middle of the early arrival window, will be most profitable.

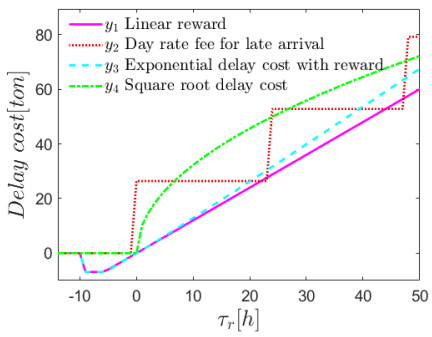

(a) Delay cost function form, where τ_r is delay time

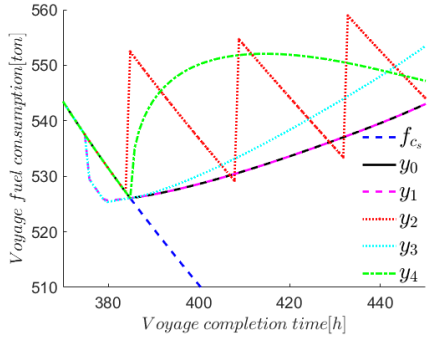

(b) Delay cost function form in statistical cost model

Figure 7.4.2

y_1 is given by:

$$y_1 = \kappa_1 \cdot \max\left(\beta, \tau_r\right) \quad \text{for} \quad \tau_r > \alpha \tag{7.4.1}$$

where κ_1 is a constant with unit tons per hour, β is the reward for early arrival with unit hours, τ_r is delay time and α is the early arrival time at which the reward starts.
y_2 is given by:

$$y_2 = \kappa_2 \cdot \max\left(0, \frac{\tau_r}{24} + 1\right) \quad \text{for} \quad \tau_r > 0 \tag{7.4.2}$$

where κ_2 has unit tons per day.
y_3 is given by:

$$y_3 = \kappa_3 \cdot \max\left(\gamma, \tau_r^{\zeta}\right) \quad \text{for} \quad \tau_r > \alpha \tag{7.4.3}$$

where κ_3 has unit tons per $hour^{\zeta}$. γ is the reward for early arrival with unit $hour^{\zeta}$. ζ exponential value for increasing delay cost.
y_4 is given by:

$$y_4 = \kappa_4 \cdot \Re\left(\sqrt{\tau_r}\right) \quad \text{for} \quad \tau_r > 0 \tag{7.4.4}$$

where κ_4 has unit tons per $\sqrt{hour}$.

β and γ can be interpreted as reward measured in fuel cost for hours of early arrival. For example, if the ship arrives 5 hours early (maximum reward in the example displayed in Figure 7.4.2b) a reward is received equivalent to 6.2 tons of fuel, which is about 21 000 NOK. If the ship arrives 2 hours early a reward is received equivalent to 2.5 tons, which is about 8 000 NOK. By changing β and γ the rewarded amount is adjusted accordingly. κ_n and ζ effects the slope of the curve. In Figure 7.4.3 an example with different κ, β and γ values are displayed.

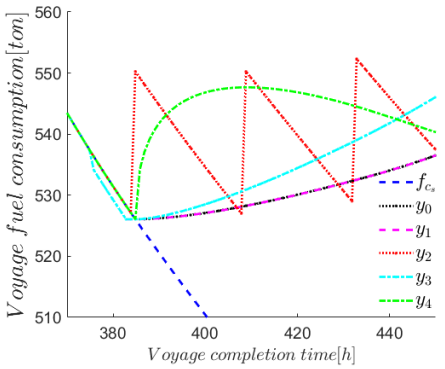

Figure 7.4.3: Statistical cost model with change in κ, β and γ

Chapter 8

Results

The horizon value, target speed, linear delay cost with rate κ and delay cost form is studied to investigate how simulated ship operation is affected by available information and decision basis. Firstly, results from the initial case is presented followed by results from the weather forecast horizon study. Lastly, results from the delay cost study is presented where target time of arrival and linear delay cost is studied followed by delay cost function form.

8.1 Initial case

A voyage from Shanghai to Panama was simulated for sea passage parameters given in Table 7.2.1 and the scenario is described in Table 7.4.1. A storm is detected on the great circle route Figure 8.1.1a. The simulated voyage chooses to go north, while the ship (OD) sailed south. The routes sailing north are chased by a storm up to the northern part of the Bering Sea, Figure 8.1.1b. Just before sailing hour 200 a drop in speed is detected. It is an attempt to wait out the storm which it has to eventually partially enter, see Figure 8.1.1c. Time series for experienced wave height, Figure 8.1.2b, displays encounter of high wave heights past 200 hours of sailing. After the storm the simulated routes again speed up, see simulation time 200+ in Figure 8.1.3. With regards to experienced wave heights, distance sailed, duration and fuel consumption the fixed calculations based on full-scale data, appear to be a better choice, see Table 8.1.1. The operational data provides us with information showing the simulated voyages are not optimal. The fixed route based on full-scale date provides better operational performance. Thus, it is questioned whether the simulator and the captain (sailing the actual ship) have access to the same information. When stating the horizon for the simulator, it limits the available information, and set an unnatural and abrupt end to information compared to reality. Based on these findings a sensitivity study for the horizon length is conducted, see Section 8.2. Further, how change in the decision basis i.e. target speed, cost function form and slope are subjects of study in Section 8.3. How these parameters can be tuned to fit different operational strategies and handle

storm encounters can help the ship owner in achieving a design suited for their strategies and operations.

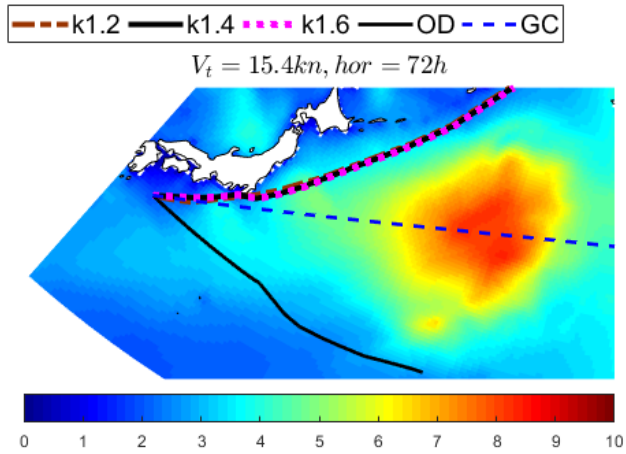

(a) Snapshot at sailing time (ts) 107 hours. A storm is situated on top of great circle route (GC). Simulated voyages sail north of the storm, while the actual ship (OD) sailed south.

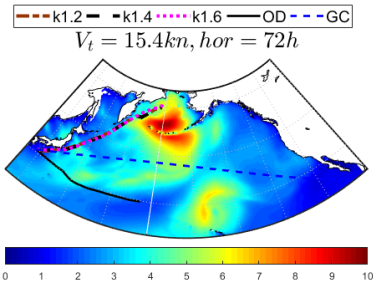

(b) Snapshot at ts 155 h. The simulated voyages encounter storm in the Bering Sea.

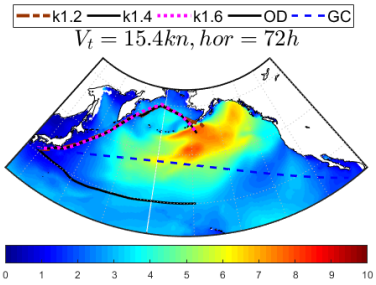

(c) Snapshot at ts 227 h. The simulated voyages are forced to sail into high waves.

Figure 8.1.1: Snapshots for simulated voyages with target speed 15.4 knots and horizon of 72 hours. OD is the fixed sailing calculations for the full-scale measurements. The simulated voyages chooses to go north while OD sailed south.

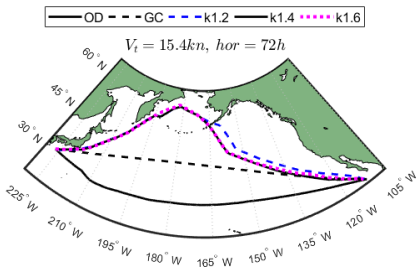

(a) Overview of selected paths.

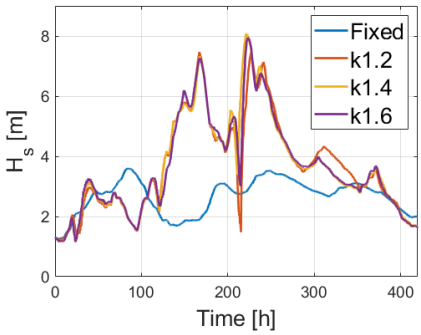

(b) Time series of H_s. The experience wave height is considerably higher for simulated voyages than fixed calculations based on full-scale data.

Figure 8.1.2: Target speed 15.4 knots and horizon of 72 hours.

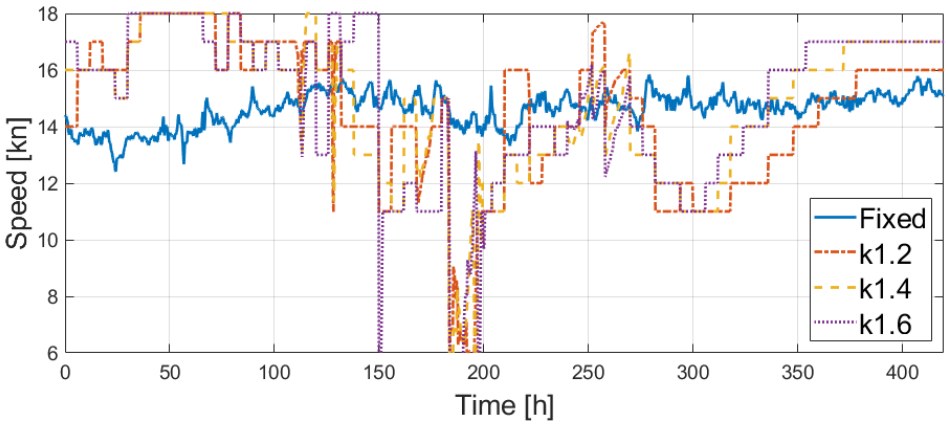

Figure 8.1.3: Time series of vessel speed. The simulated voyages experience considerable speed loss with storm encounters, whereas OD maintain a steady speed profile. Target speed 15.4 knots and horizon of 72 hours.

8.2 Length of horizon

A sensitivity study for the horizon length is conducted on a voyage from Shanghai to Panama and a voyage from Shanghai to Seattle, described in table 7.3.1. The horizon is varied from 48 hours to 120 hours, with sea passage model parameters as described in Table 7.2.1.

Table 8.1.1: Scenario results overview for original linear kappa study vt 15.4 hor 72 hours

Case vt15.4	Distance [nm]	Duration [h]	Average speed [kn]	mean %MCR [%]	std [%]	Fuel consumption [ton]	Fuel con. rate [ton/day]	mean Hs [m]
OD	6131	420	14,6	78,4	1,7	519	30	2,7
Fixed	6131	420	14,6	49,9	8,6	485	28	2,7
k1.2	6385	438	14,6	55,9	15,4	560	31	3,6
k1.4	6389	432	14,8	57,3	16,3	567	32	3,6
k1.6	6408	432	14,8	57,2	16,7	568	32	3,6

8.2.1 Shanghai Panama

A voyage from Shanghai to Panama with scenarios as described in Table 7.4.1 were simulated and compared to full-scale measurements. Simulated voyages with horizon up to 96 hours choose to sail north of the storm detected on great circle route, fig. 8.2.1a, while horizon 120 hours and OD sailed south of the storm.

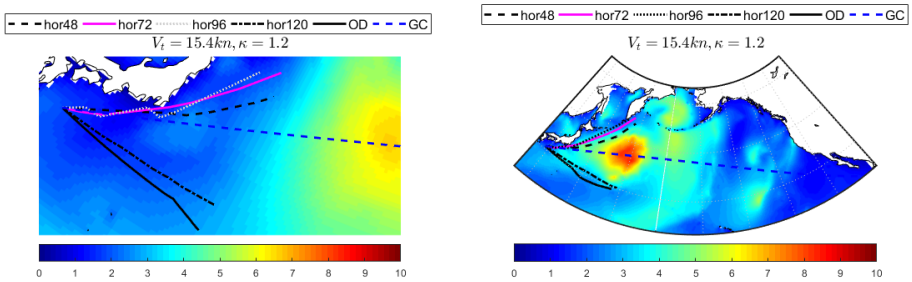

(a) Snapshot at ts 59 hours. With an horizon of 120 hours the sea passage model sail south, same as OD.

(b) Snapshot at ts 107 hours. Hor72 has sailed longer than hor48 and hor96. Hor120 is ahead of OD.

Figure 8.2.1: Snapshots for simulated voyages with target speed 15.4 knots. With varying horizon from 48 h to 96 h.

In Figure 8.2.1a it is observed that hor96 shows tendencies of indecisiveness, and have abrupt heading changes 4 times before it heads north as hor48 and hor72. Based on this there were reasons to suspect that hor96 were close do detecting the better option of going south. In Figure 8.2.3a it is displayed that considerable lower wave heights are encountered when sailing south of GC. In Figure 8.2.3b we see that hor120 do not have the same reductions in speed as the simulated routes that sail south of the GC.

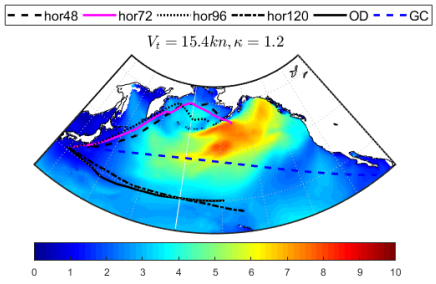

(a) Snapshot at ts 227 hours. Hor72 have entered an area with high waves. Hor120 have gained additional advance on OD in distance and sails more south than OD.

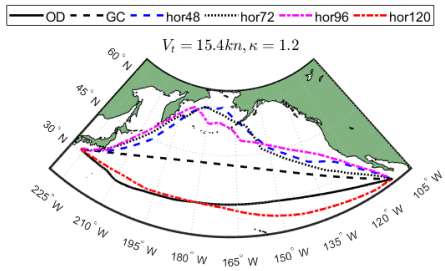

(b) Overview of selected paths.

Figure 8.2.2: Snapshots for simulated voyages with target speed 15.4 knots. With varying horizon from 48 h to 96 h.

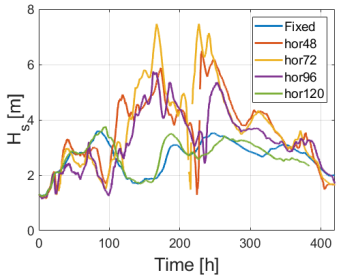

(a) Simulated voyage for horizon up to 96 h experience considerably higher wave heights than simulated voyage with horizon 120 and OD.

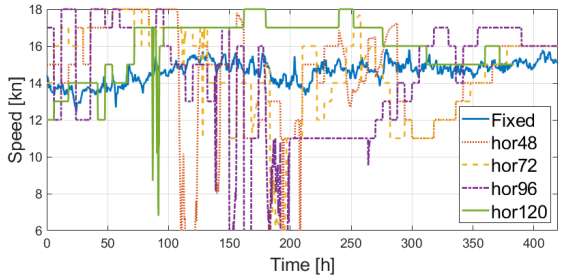

(b) Hor120 maintains similar speed as OD up to ts 50 h. A considerable speed reduction is observed around ts 100 for hor120. After ts 100 h hor120 maintain on average a higher speed than OD.

Figure 8.2.3: Time series of H_s and vessel speed for V_t=15.4 kn, varying horizon and κ=1.2.

To further investigate the limit for sailing north versus south, the horizon was discretized into 6 hour intervals from 102 hours to 114 hours, see Figure 8.2.5. The boundary was found to be between hor96 and hor102. For hor102 to hor114 we see routes going south due to the detected storm situated on the great circle route. We see our simulation stays in a dark blue area, close to where it turns cyan, fig. 8.2.4a, whereas OD choose to sail a bit further south. At simulation hour 167 the simulated routes are in front of OD, and the routes have coincided, fig. 8.2.4b. For simulation hour 251 the simulated routes are well in front of OD and head further south. The simulated routes stay in an area with darker blue than OD,

which may be the reason for heading further south. From time series of H_s it is observed that encountered wave height is converging for increasing horizon length, section 8.2.1. From vessel speed time series it is observed that simulated routes obtain generally higher speed than OD, which also can be seen from contour plots during sailing, fig. 8.2.5, where the simulated routes are situated further east than OD. A drastic speed loss for hor114 just before simulation hour 100 is displayed in Section 8.2.1. Almost the same wave height for all scenarios are observed at the same time, but only hor114 experiences the drastic drop in speed.

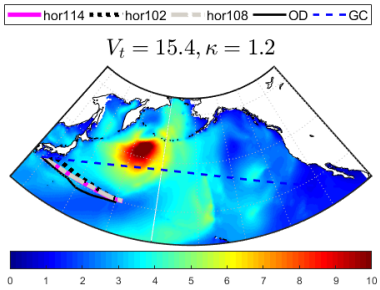

(a) Snapshot at ts 119 h. Hor102 stayes closer to GC in the beginning and then join hor108 and hor114.

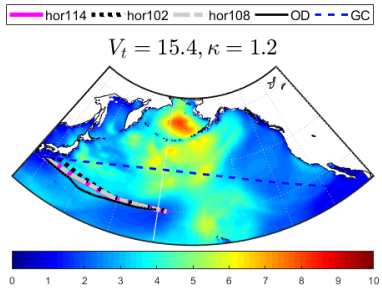

(b) Snapshot at ts 167 h. The path for OD and simulated voyages coincides.

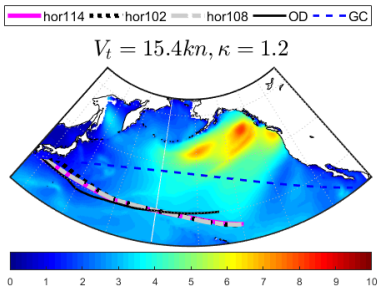

(c) Snapshot at ts 251 h. The simulated voyages is ahead of OD, indicating that they maintain a higher average speed

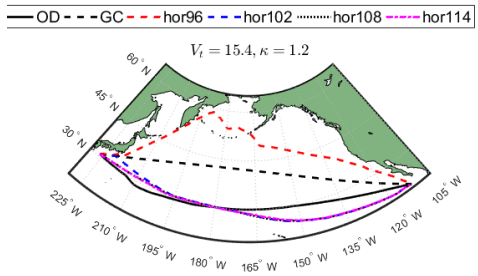

(d) Overview of selected paths.

Figure 8.2.4: Snapshot of sea passage routes for target speed of 15.4 knots and horizon varying from 102 h to 114 h.

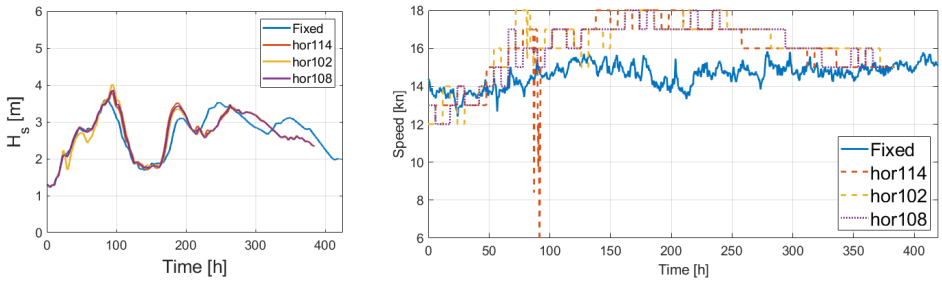

Figure 8.2.5: Time series for H_s and vessel speed for V_t=15.4 kn and horizon from 102 h to 114 h. Similar encountered wave heights for fixed calculations based on full-scale data and simulated voyages. The simulated voyages maintain generally an higher speed than fixed calculations.

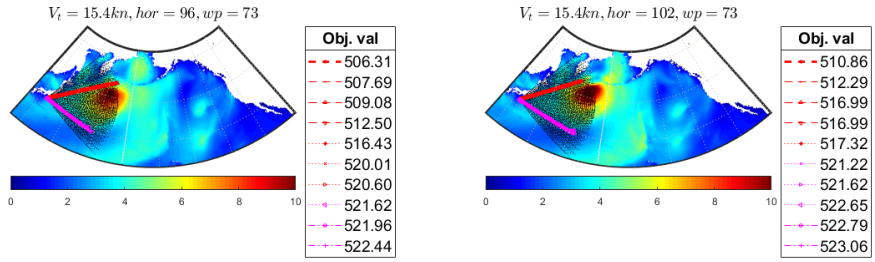

(a) Snapshot of candidate routes at wp 73 for hor96. The ten best options are split in two. The seven best options points north of GC (in red) and the rest points south (in pink). A significant difference in heading of around 30 degrees are observed. Red candidate stretches farthest.

(b) Snapshot of candidate routes at wp 73 for hor102. Also here the ten best options are split in two. Similar speed is proposed since they stretch about the same length. Objective values are higher than for hor96 which is natural since the candidate routes cover a larger time horizon.

Figure 8.2.6: Snapshot of waypoint 73 candidate routes for hor96 and hor102, with target speed 15.4 knots and κ 1.2

In Figure 8.2.6 and Figure 8.2.7 the candidate routes and appurtenant objective values are displayed. At waypoint 73, the ten best options are split in two for both hor96 and hor102. The options that head north tend to involve higher speed since the route stretches further than the ones going south. At waypoint 97 both hor96 and hor102 have the ten best options south of the storm, see Figure 8.2.7a and Figure 8.2.7b. At waypoint 121 a crossroads is found for hor96 and hor102, see Figure 8.2.7c and Figure 8.2.7d, where hor96 have all ten best options north of the

GC and hor102 have all ten best options south of the GC. Thus, the length of the horizon is found to have significant impact on selected route.

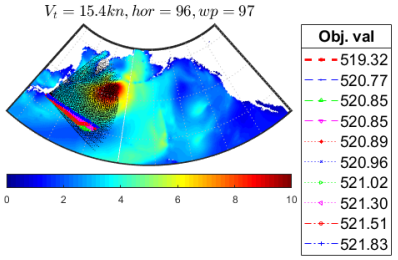

(a) Snapshot of candidate routes at wp 97 for hor96. All ten best options point south of GC at this waypoint

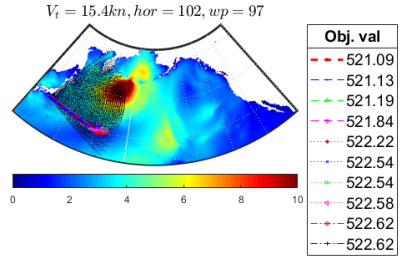

(b) Snapshot of candidate routes at wp 97 for hor102. All ten best options point south of GC at this waypoint

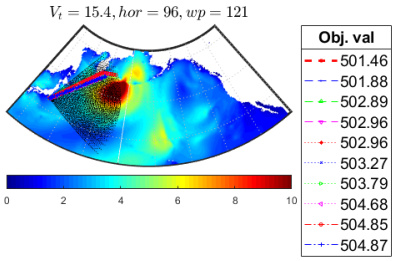

(c) Snapshot of candidate routes at wp 121 for hor96. The ten best options now points north again as for wp 73.

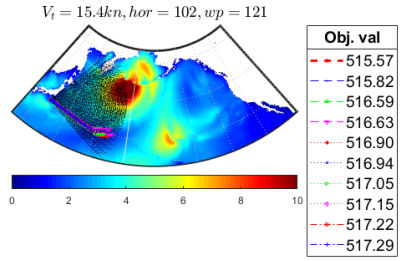

(d) Snapshot of candidate routes at wp 121 for hor102. The ten best options continuous to be south of the GC.

Figure 8.2.7: Snapshot of candidate routes during start of voyage for hor96 and hor102, with target speed 15.4 knots and κ 1.2

In Table 8.2.1 an overview of the operational parameters for all scenarios including OD and Fixed results are displayed. For horizon lenghts up to 96 hours, the simulated voyages arrive late, while for horizon 102 and above arrive early. Hor108, hor114 and hor120 sails about the same distance but with 1.4 knots higher average speed. The standard deviation for propulsion power %MCR are significantly lower for hor102 and above, indicating more steady loading conditions, than what is obtained for hor96 and below. Standard deviation for propulsion power %MCR for hor102 and above is similar to what is obtained for Fixed. Mean H_s is equal for OD, Fixed, hor102 and above. For hor96 and below mean H_s vary from 3.1 meters up to 3.6 meters.

Table 8.2.1: Scenario result overview horizon study for V_t=15.4 kn Shanghai Panama

Case $v_t15.4\kappa1.2$	Distance [nm]	Duration [h]	Average speed [kn]	mean %MCR [%]	std [%]	Fuel consumption [ton]	Fuel con. rate [ton/day]	mean Hs [m]
OD	6131	420	14,6	78,4	1,7	519	30	2,7
Fixed	6131	420	14,6	49,9	8,6	485	28	2,7
hor 48	6366	438	14,5	58,0	18,8	585	32	3,5
hor 72	6385	438	14,6	55,9	15,4	560	31	3,6
hor 96	6384	450	14,2	50,1	18,5	520	28	3,1
hor102	6178	384	16,1	56,4	9,7	498	31	2,7
hor108	6126	384	16,0	55,1	9,0	487	30	2,7
hor114	6130	384	16,0	55,2	9,3	488	30	2,7
hor 120	6126	384	16,0	55,0	8,8	486	30	2,7

8.2.2 Shanghai Seattle

A voyage from Shanghai to Seattle was simulated for sea passage parameters given in Table 7.2.1. A scenario description is found in Table 7.4.1. In Figure 8.2.8a we see that there is a storm situated just below the great circle route causing OD to slow down and go south. hor96 and hor120 stay close to the great circle route but do not maintain as high speed as hor48 and hor72 that go north of the great circle route. At simulation houre 157 hor96, hor120 and OD catches up with hor48 and hor72 and all scenarios are now closing in on the great circle route towards the destination. The experienced wave height, see Figure 8.2.9a, are similar for hor96 and hor120, since they follow approximately same path. OD, hor48 and hor72 experience overall higher sea states than hor96 and hor120. Speed is mainly below OD for hor96 and hor120, while it is both below and above for hor48 and hor72, see Figure 8.2.9b.

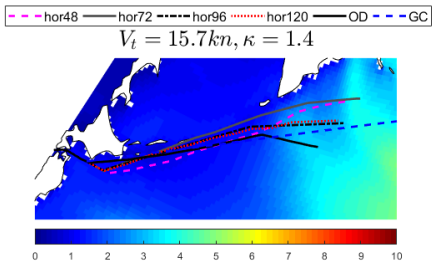

(a) Snapshot at ts 61 h. hor120, hor96 and OD stay relatively close to GC.

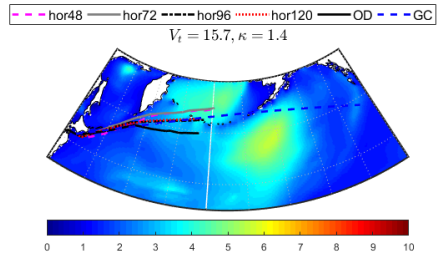

(b) Snapshot at ts 67 h. hor48 and hor96 go north of GC, hor96 and hor120 stay relatively close to GC and OD sail south of GC.

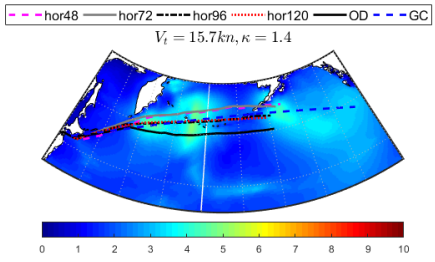

(c) Snapshot at ts 157 h.

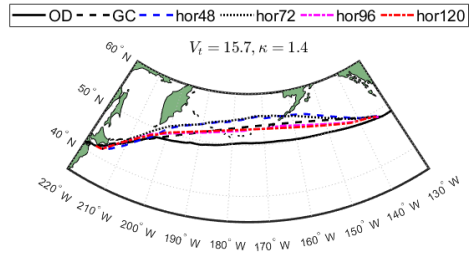

(d) Overview of selected paths

Figure 8.2.8: Snapshot of sea passage routes from Shanghai to Seattle for target speed of 15.7 knots and horizon varying from 48 h to 120 h.

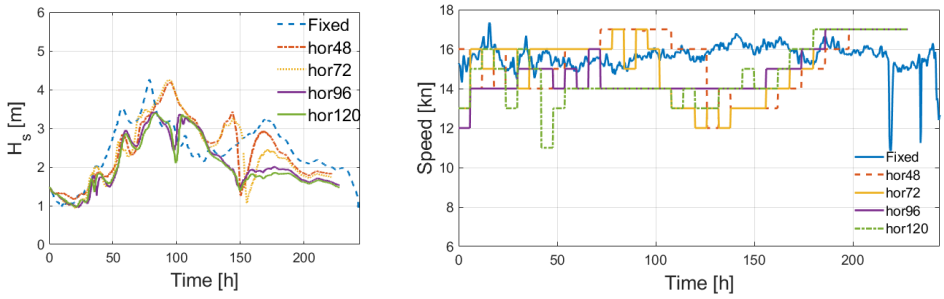

(a) (b)

Figure 8.2.9: Time series of H_s and vessel speed for V_t=15.7 knots, κ=1.4 and varying horizon from 48 h to 120 h.

Table 8.2.2: Scenario result overview horizon study for vt15.7 Shanghai Seattle

Case vt15.7	Distance [nm]	Duration [h]	Average speed [kn]	mean %MCR [%]	std [%]	Fuel consumption [ton]	Fuel con. rate [ton/day]	mean Hs [m]
OD	4010	257	15,7	82,6	1,7	337	32	2,4
fixed	4010	257	15,7	53,1	5,5	296	29	2,4
hor 48	3396	222	15,3	50,1	8,7	257	28	2,4
hor 72	3354	222	15,1	48,5	9,6	249	27	2,4
hor 96	3384	228	14,8	46,1	9,3	244	26	2,1
hor 120	3360	228	14,7	45,3	10,3	240	25	2,0

8.2.3 Summary

The horizon length can potentially affect the selected route significantly. Encountered wave height converge for horizon length above 102 hours. With a longer horizon, the operational performance is generally improved for all cases. Since the arrival time for hor102 and above is 36 hours before OD, it is interesting to see if arriving at same time will make the simulated routes and OD coincide further.

8.3 Delay cost

The schedule is set by the target speed and great circle route at initiation. During simulations the cost function restricts the simulator by adding a cost for delays. The simulator can choose to change vessel speed and heading, and thereby path of sailing. A case study on how decisions basis affect route and performance is presented in this section. By decision basis the terms on which the sea passage simulator makes decisions are meant, i.e. minimum fuel consumption and delay cost.

8.3.1 Target speed and linear delay cost

To study how the decision basis affect the simulated operations, a case study where the target speed and linear delay cost with rate κ is increased. Scenarios are described in table 7.4.1. Behaviour in calm seas and when encountering storms are of interest. Hence, horizon of 72 hours and 120 hours for the Shanghai Panama route was selected. Target speed 14.1 knots is based on ship arrival for full scale data, whereas 15.4 knots is the statistical required average speed based on the statistical model, see Table 7.4.2. Target speed of 16.4 knots is selected to see how further increase is handled. Table overview of operational parameters for all scenarios can be found in Appendix B. Only a few selected table overviews is given here for illustration purposes.

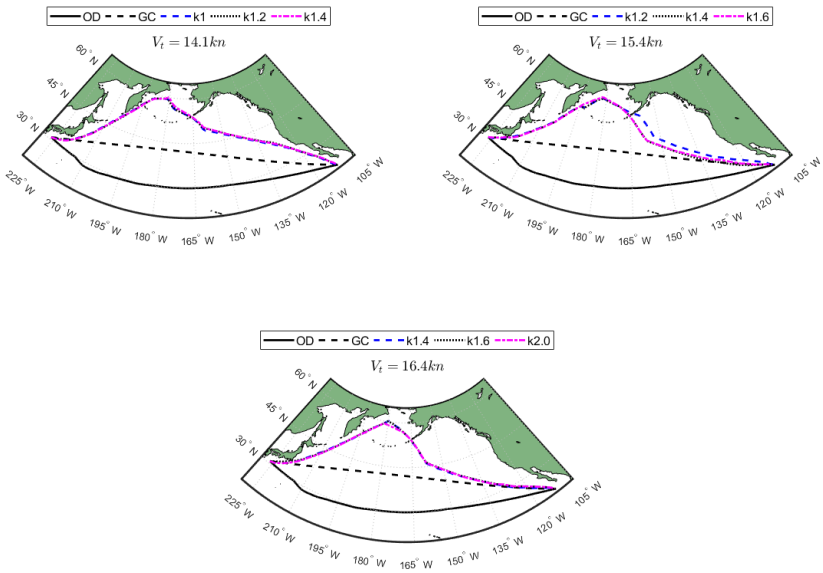

Figure 8.3.1: Voyage routing for varying speed and linear slope value κ. Paths for κ 2 and κ 1.6 is overlapping, hence it is hard to see κ 1.6

In Figure 8.3.1 we see the routes tend towards great circle route for increasing target speed V_t. With increasing target speed and/or increasing κ the simulator will balance increased speed, and thus fuel consumption, increased distance (by sailing around the storm) against sailing trough the storm and/or waiting out the storm by reducing speed. In hor72 distance increases for increasing κ, see table 8.3.1, which is a result of the simulator speeding up and trying to drive around the storm. Mean %MCR, fuel consumption and H_s increases. The increased mean H_s is due to increasing κ finds it more profitable to enter bad seas, versus arriving late.

Table 8.3.1: Scenario result overview for original linear kappa study for V_t= 14.1 kn and horizon of 72 h

Case vt14.1	Distance [nm]	Duration [h]	Average speed [kn]	mean %MCR [%]	std [%]	Fuel consumption [ton]	Fuel con. rate [ton/day]	mean Hs [m]
k1	6377	468	13,6	45,2	14,4	492	25	3,0
k1.2	6382	456	14,0	48,0	16,6	507	27	3,1
k1.4	6407	450	14,2	50,1	18,5	522	28	3,1

For relatively calm seas, as experienced with horizon of 120 hours on the Shanghai Panama route, and horizon 120 for Shanghai Seattle route, the selected path and operational parameters varies little. This is because it is not delayed due to bad seas. With horizon of 120 hours and target speed 14.1 we see the simulated routes duration and speed is similar to those found for Fixed calculations for that route. The simulated routes sail a shorter distance, consume less fuel and obtain mean %MCR below Fixed, about the same std as Fixed and similar mean H_s. Generally increased κ leads to increased distance and increased speed, if a storm is encountered during sailing. While increasing target speed leads to decreasing distance (willingness to go though rougher seas to reach destination in time) and thus tends towards great circle route.

Table 8.3.2: Scenario result overview for original linear kappa study vt 14.1 hor 120 hours

Case vt14.1	Distance [nm]	Duration [h]	Average speed [kn]	mean %MCR [%]	std [%]	Fuel consumption [ton]	Fuel con. rate [ton/day]	mean Hs [m]
k1	6090	420	14,5	45,1	7,9	440	25	2,7
k1.2	6078	414	14,7	46,5	7,5	447	26	2,7
k1.4	6168	420	14,7	46,5	8,0	453	26	2,7

To test the hypothesis that increased κ in calm seas do not affect operational parameters noticeably was tested for Shanghai Panama with target speed 15.4 knots and horizon of 120 hours, and can be found in Appendix B. Only minor differences which is natural due to the genetic algorithm used for speed optimisation is present.

8.3.2 Delay cost function form

The delay cost in the objective function represents the consequences of schedule disruption. Depending on the ships mode of operation delayed arrival may lead to contracted fees for delayed cargo, extra cost for crew and cargo handling, schedule disruption and lost day-rate income. Five types of cost functions are tested in the simulator. A description of each function can be found in Section 7.4.2. In Figure 7.4.2 the different functions are displayed in the statistical cost function model. For the functions rewarding early arrival half the expenses for arriving maximum early contra arriving on time is given as reward for early arrival. I.e. arriving in the middle of the early arrival window will be most profitable. The target time of arrival with target speed 14.1 knots is 420 hours. The Shanghai Panama route with target speed 14.1 knots is simulated with horizon 96 hours and 120 hours for all cost functions and presented in the following subsections.

Horizon 120 hours

y_0, y_2 and y_4 arrive on time while y_1 and y_3, rewarding early arrival, arrive 6 hours early. This gives approximately little under maximum reward. y_4 and y_2 maintain the highest average speed and is the functions with the steepest slopes. y_2 has the highest fuel consumption followed by y_4 and y_2. y_1 arrives early but manage to perform second best on fuel consumption and maintains the second lowest average speed, same as OD and Fixed.

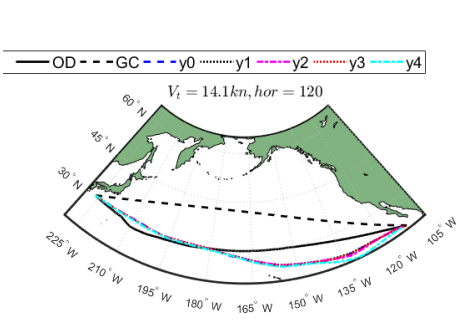

(a) All simulated paths are south of GC and coinciding.

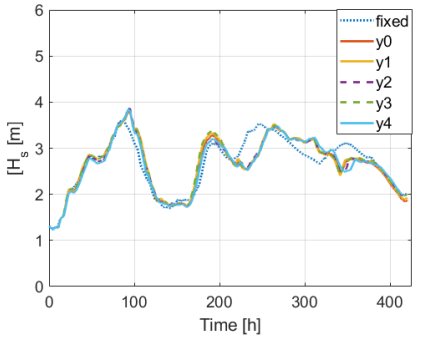

(b) Time series H_s. Encountered wave height is similar for simulated routes and fixed route based on full-scale data.

Figure 8.3.2: Route and time series of H_s for V_t=14.1 kn and horizon 120 h

Table 8.3.3: Scenario result overview for horizon study with V_t=14.1 kn and horizon 120 h. Route: Shanghai Panama

Case vt14.1	Distance [nm]	Duration [h]	Average speed [kn]	mean %MCR [%]	std [%]	Fuel consumption [ton]	Fuel con. rate [ton/day]	mean Hs [m]
OD	6131	420	14,6	78,5	1,7	519	30	2,7
Fixed	6131	420	14,6	49,9	8,6	485	28	2,7
y0	6090	420	14,5	45,1	7,9	440	25	2,7
y1	6114	420	14,6	45,8	8,4	447	26	2,7
y2	6107	414	14,8	46,8	8,1	450	26	2,7
y3	6168	420	14,7	46,4	8,0	453	26	2,7
y4	6090	414	14,8	46,5	8,3	447	26	2,7

Horizon 96 hours

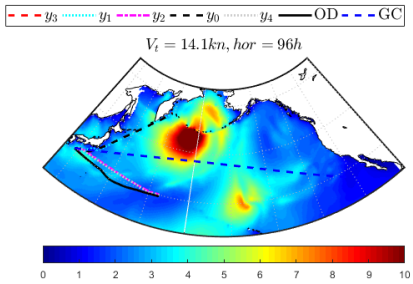

(a) Snapshot at ts 131 h. y_2 and y_4 sail south while y_0, y_1 and y_3 sail north.

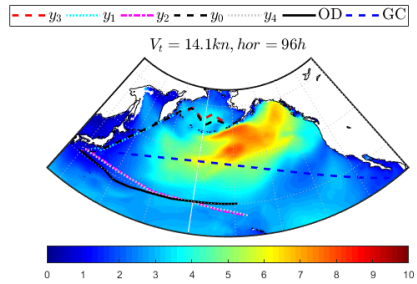

(b) Snapshot at ts 227 h. y_2 and y_4 is a bit ahead of OD. y_0, y_1 and y_3 encounter a storm in the north.

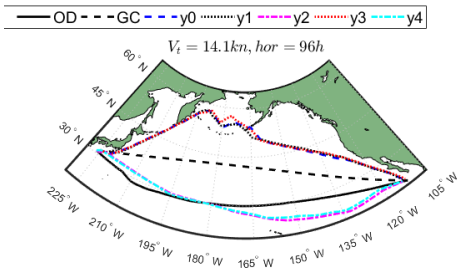

(c) Overview of selected paths

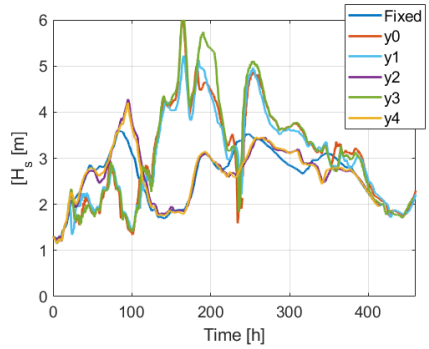

(d) Time series of H_s. The routes that sail north encounter higher wave heights.

Figure 8.3.3: Sea passage routes for target speed of 14.1 kn and horizon of 96 hours with different cost functions. Route: Shanghai Panama

y_2 and y_4 which is the two functions with the steepest slope choose to sail south of the great circle route with horizon length 96 hours. The original delay cost with rate κ did not choose to sail south for same target speed for κs up to 1.4. Hence, the cost function assist in the strategic decision of going south. As a result y_4 and y_2 experience significantly lower wave heights, see Figure 8.3.3d, and arrive 6 hours early, see Table 8.3.4. y_4 and y_2 do not reward early arrival. The average speed for the two functions are reported to be 0.7 knots higher than target speed, but obtain the lowest fuel consumption due to the low encountered wave heights. Form time series of vessel speed, Figure 8.3.4, it is observed that y_4 and y_2 maintain a lower speed than y_0, y_1 and y_3 for the first 70 hours of sailing. The first 70 hours are also considered to be part of the critical part for path selection, and may be a contributing factor to that they choose to go south.

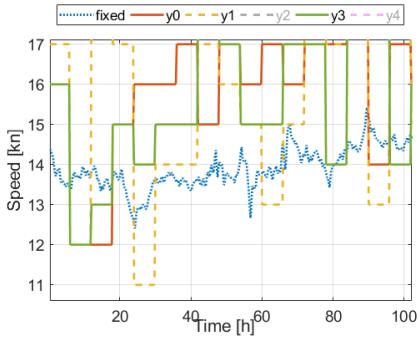

(a) Time series of vessel speed for cost function y_0, y_1 and y_3

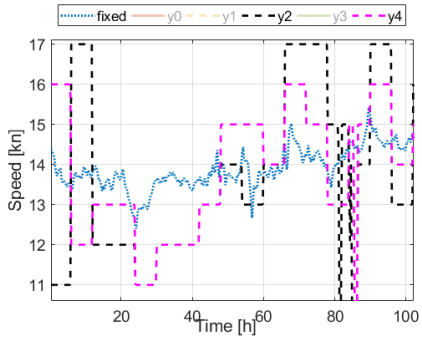

(b) Time series of vessel speed for cost function y_2 and y_4

Figure 8.3.4: Time series of vessel speed for V_t 14.1 kn and horizon 96 h.

Table 8.3.4: Scenario result overview horizon study for V_t=14.1 kn and horizon 96 h. Route: Shanghai Panama

Case vt14.1	Distance [nm]	Duration [h]	Average speed [kn]	mean %MCR [%]	std [%]	Fuel consumption [ton]	Fuel con. rate [ton/day]	mean Hs [m]
OD	6131	420	14,6	78,5	1,7	519	30	2,7
Fixed	6131	420	14,6	49,9	8,6	485	28	2,7
y0	6432	462	13,9	46,6	14.6	499	26	3,0
y1	6340	462	13,7	46,5	16,4	498	26	3,0
y2	6129	414	14,8	47,6	10,1	457	26	2,7
y3	6458	456	14,2	49,7	17,1	523	28	3,1
y4	6432	414	14,8	47,5	9,1	455	26	2,7

8.3.3 Summary

By varying the basis of which decisions are made, different combinations of vessel path and speed is achieved. Increasing target time may generally lead to the selected path tending towards the great circle route. Increasing linear delay cost

may lead to increased distance and speed if a storm is encountered, as a consequence of speeding up and sailing around the storm (and/or slowing down to wait out the storm and afterwards speeding up) to arrive with minimum delay cost. Cost function form can affect both speed and vessel path, and help in strategical decision making.

8.4 Computational time

A table with all computational time for scenarios presented in this study can be found in Appendix C. The average time is 17.9 seconds per way point and the standard deviation is 4.9. The minimum time is 10.7 seconds per way point and the maximum time is 26.0 seconds per way point. On average it takes 8.4 hours to simulate a voyage from Shanghai to Panama and it takes on average 4.2 hours to simulate a voyage from Shanghai Seattle. Due to variation in speed, kappa, hor and cost function, the duration and distance travelled vary and thus computational time vary as well, as is displayed by the high standard deviation.

Chapter 9

Discussion

This chapter presents the discussion on methods and assumptions applied in this thesis. The aim is to clarify the validity of the approach and findings from this case study.

9.1 Conceptual model validation

With regards to theories and assumptions underlying the conceptual ship model the biggest uncertainty is believed to be in the resistance calculations and power estimates. Air resistance, current and increased resistance due to manoeuvring is not included in the ship model and are thus sources of error. The draught is held constant and set to 10.5 meters. The measured draught for full-scale measurements are smaller for both comparison routes. For the general cargo carrier design applied in this thesis, calm water resistance test, open water characteristics and propulsion tests were available. They are considered to be of high quality. For added resistance in waves the generalised approach of Gerritsma and Beuklman by Lukakis and Sclavounos covering oblique waves is applied. Stern- and stern-quartering wave added resistance estimates for this method contains uncertainty. For beam-sea (90 ° angle of attack) to stern-sea, added resistance is mostly estimated to give negative contribution. To avoid large negative contributions that are unrealistic from the simulator all negative contributions were set to 0. From studying Figure 6.3.4a a large underestimation of resistance is found for bow-quartering to stern-seas. If negative contributions where included, the underestimations would have been even larger. Thus, model validity gradually decreases from bow-quartering seas to stern-seas. Further, the model validity decrease for high sea states as well as the combination of medium sea states and low speed, fig. 6.1.2. For estimation of specific fuel oil consumption, a shop test for the installed machinery is used. Machinery modelling is a complex task and is very simplified in this model and therefore contains uncertainties. Short term statistics are based on the standard wave spectrum Pierson-Moskowie and is suitable for a fully developed wind-driven sea, where the wind has been blowing long enough over a large area and waves that

are generated elsewhere do not enter. For long term wave statistics distribution parameters for world-wide operation of ships is applied. These are valid for among others USA West coast and Japan.

9.2 Historical data validation

Calm water resistance was initially based on a calm water model test and then corrected for ideal circumstances during test by comparing with calm sea data points in full-scale data. No data related to weather conditions other than relative wind speed is sampled for the full-scale data, thus the assumption of calm seas depends entirely on this. Resistance contributors such as waves, wind and current are most likely present, and not accounted for when doing this correction. The reason for correcting the calm water resistance curve was due to the sensitive relation between speed and power. Large variations in power was observed for model results while full-scale data did not display the same variation in amplitudes. The variations were traced to the calm water resistance calculations. Before correction the model on average overestimated the power, while it underestimated fuel consumption. After correction, an almost linear resistance curve was proposed. The corrected model displayed behaviour for wave attack angles below 50 ° similar to full-scale data. Based on full scale data it is found to underestimate on average, which is in correlation with what we see when comparing OD to Fixed calculation (by ship model) in Table 6.3.2. Here mean %MCR is about 29 % lower for Fixed than OD for the route from Shanghai to Panama. The standard deviation was reduced for both routes for the corrected model compared to the initial model. The fuel consumption curve is increased with about 25 % compared to the initial model but still underestimates more than what is observed for the initial model. Fuel consumption is dependent on power, and therefore the underestimation of power is aggregated in to the fuel consumption estimates. Power estimates are essential for operational performance. For testing ship design in reality, the accuracy of propulsion power estimates and thus fuel consumption is considered to me too low, but that is not the main objective for this thesis. When correcting the calm water resistance curve and specific fuel oil curve, a higher number of data points with known wave conditions could increase validity of the correction.

9.3 Simulated ship operation

The aim here was to model navigational decisions within the framework of tactical decisions where one travels from A to B with a given design. The process of simulating ship operation and the learning outcome is discussed below.

9.3.1 Table look-up modelling

A table look-up data set with combinations of sea states, wave directions and vessel speeds were created with a MATLAB script combining model test results for calm

water resistance and propulsion power with quasi-static wave added resistance estimates from ShipX Veres. In addition, Operability limiting criteria were conducted in ShipX for the voluntary speed reduction criteria. Hence, it is assumed that characteristic steady-state values are present for the duration of the sea state. Sailing is in reality a dynamic process with transient loading in varying sea states.

9.3.2 Human factors

To make an optimal decision, you have to:

1. have necessary information available
2. be able to assemble the information and analyse it to identify optimal choice
3. be able to make the right decisions given you are able to see the optimal choice

It is both relevant for a human captain sailing a ship and a computerised simulation trying to virtually sail a ship. A captain is limited by ship capabilities, available information on the bridge, available weather forecasts and ship owner requirements to the captain. How the captain interprets and manage the given information will affect the ships operation. A computerised model will be limited by applied theories, assumptions and inputs to the model. The motivation behind the sea passage model is to "improve relevance for virtual testing sea passage scenarios by controlling how the vessel model executes its voyage." (Sandvik et al. n.d.). In order to improve relevance a replication of available information for a real human captain must be considered and modelled mathematically. Humans are individuals and will have distinctive characteristics that are hard to replicate, and sometimes also unwanted. The sea passage model will make optimal decisions based on the available information, within the observed horizon and routing discritization. Given the required information a human will not necessarily make optimal choices. The sea passage model therefore represents an abstraction, i.e. something which only exists as an idea.

9.3.3 Boundaries for rationality

Weather forecasts are subject to uncertainty, and generally a function of lead time between forecast issuance and time of realisation. This uncertainty is neglected in the model. Hindcast data is used as forecast, thus ensuring the model is able to make the best decisions possible within the observed horizon. A ship sailing in reality is subject to this uncertainty. In the model an abrupt end to available information follows the end of the horizon. This limits the simulators ability to make strategic routing decisions, whereas a human captain would process the forecast and uncertainty beyond this point, and therefore have a greater strategic decision ability.

9.3.4 Available information

To model all available information for a real human captain is a complex task, and therefore a balance between what is strictly speaking required and what is not. An attempt is therefore made to compare the sea passage model with full-scale data to reveal unevenness with regards to available information. After conducting initial simulations for a voyage from Shanghai to Panama in January it was uncovered that the simulated voyages chose to sail north whereas the full-scale data ship actually sailed south. Hence, it was questioned whether the simulator had access to sufficient amount of information compared to a captain sailing a ship in reality. Due to statistically rougher wave climate and occurrence of sea ice in arctic regions, a captain is most likely reluctant to go as far north as the simulated routes suggest during fall and winter. This is subjective considerations, dependent on experience and preferences. Time series of the experienced wave height were significantly higher than for the route selected by the full-scale ship. Based on this information it could be established that the sea passage simulator did not perform optimal with the given parameters in the initial case, and a better route could be found south of the great circle. The length of the horizon and the abrupt end to available information at the end of the horizon was suspected to limit the ability for strategic routing decision below what we could seemingly expect from a human captain.

A sensitivity study on the horizon length was conducted and it was found that the sea passage model sailed south with a horizon of 102 hours, and that experienced wave height converged from 102 hours to 120 hours for the Shanghai Panama route. For Shanghai Seattle the simulator also chose to go north for horizon up to 72 hours, and horizons 96 to 120 moved towards the great circle route, whereas the ship sailed south of the great circle route. Encountered wave height converge from horizon 102 hours and upward for Shanghai Panama and from 96 hours and upwards for Shanghai Seattle. Hence, how the horizon is modelled affects the selected route significantly. For the case study conducted in this research, indications that a human captain has a weather horizon of at least 96 hours. In Janssen & Bidlot (2018) it is found that weather forecasts up to 5 days ahead is of good quality. Introducing uncertainty in weather forecast and thus removing the abrupt end to available information at end of horizon should be considered for future development.

9.4 Delay cost

In the economical domain a ship is a mode of transport for cargo were ship owners and operators strive to reduce costs and increase income. The delay costs in the objective function represents the consequences of schedule disruption. Depending on the ship's mode of operation, delayed arrival may lead to contracted fees for delayed cargo, extra cost for crew and cargo handling, schedule disruption causing a knock on effect for future vessel and fleet scheduling, resulting in lost day-rate income (Aydin et al. 2017). In the sea passage model the delay cost is modelled

as a function of delay time and may be interpreted in several ways. Agreements between ship owners and cargo owners may state time windows for cargo delivery and pick-up (Christiansen et al. 2013) and/or agreements between ship owners and a captain may state financial conditions based on arrival time for the captain's salary (Li et al. 2016). Also it might be considered as available slack on subsequent voyages, (Sandvik et al. n.d.).

To get a better understanding of how target time and delay cost affected the simulations, a study was conducted on how target speed and linear delay cost with rate κ influence route selection and operational parameters. By varying these parameters different combinations of vessel path and speed is achieved. It is however dependent on if harsh weather is present along the route or not. Generally, increased κ leads to increased distance and speed if a storm is encountered during sailing. This is a result of the simulator trying to speed up and drive around the storm or wait out the storm by temporarily slowing down before again increasing when the storm has past. Increasing κ if voyage is through calm seas do not affect operational parameters noticeably, because it is not in danger of experiencing delay cost. Increasing target speed leads to decreasing distance (willingness to go through rougher seas to reach destination on time) and thus tends towards the great circle route.

Further, an attempt of creating general cost function forms, representing agreements between ship owners and cargo owners, as well as ship owners and a captain, was proposed and implemented in the sea passage model. Five different functions were tested and is described in section 7.4.2. Contracts and financial conditions for the voyage have to be known to acquire a more accurate result. The different functions can be altered to fit customers and are presented on a general basis for this study. It is found to be an efficient way of manipulation behaviour, but it should be handled with care due to its effect on operational performance, and thus may lead to erroneous interpretation of vessel performances. The function form used to model delay costs may help the sea passage model's ability to make strategic routing decisions. With two of the proposed cost functions the sea passage model managed to go south at horizon length of 96 hours, whereas the linear delay cost needed a horizon length of 102 hours to register the fact that going south was a better option than going north. Rewarding early arrival is a good way of avoiding schedule disruption within reasonable limits.

9.4.1 Computational time

Computational time is important with regards to applicability. A low computational time could allow for life cycle simulations, rapid iterations and trial-and-error by the user (designer). At the moment the average computational time for a voyage between Shanghai and Panama is around 8 hours for the total trip and 17.9 seconds per way point with a standard deviation of 4.2 seconds per way point. The standard deviation is quite high due to the varying speed, horizon, κ and cost functions applied to the case study. The grounds on which to compere these values

are therefore questionable. The sea passage model applies a genetic algorithm for speed optimization, and this increase computational time. A life cycle simulation would require improvements to the code. Parallel programming for loops does however make it possible to run several simulations at the same time. There is a trade-off between computational time and simulation study scope.

Chapter 10

Conclusion

The presented work illustrates the importance of available information and decision making in simulation-based ship operations by use of a sea passage model proposed by Sandvik et al. (n.d.). The sea passage model decision basis relies on the ability to forecast ship behaviour, thus ship model validation is considered to be of importance. It was found to be accurate enough for this purpose but containing significant uncertainties from bow-quartering seas to stern-seas. It is also found to generally underestimate power. By comparing full-scale measurements to simulated voyages important aspects and limitations with the sea passage model was uncovered:

1. The available information with regards to weather forecasts, and the abrupt end to available information and the end of the horizon is proven to be of great importance for the selected path. The sea passage model's ability to make strategic routing decisions is strongly dependent on how the horizon is modelled. For the case study conducted in this research, indications that a human captain has a weather horizon of at least 96 hours.
   Recommendation: A model where uncertainty in weather forecasts with a gradually fading horizon is therefore recommended if further development of the sea passage model shall be conducted.

2. By varying the basis of which decisions are made, different combinations of vessel path and speed is achieved. Increasing target time may generally lead to selected path tending towards the great circle route. Increasing linear delay cost may lead to increased distance and speed if a storm is encountered, as a consequence of speeding up and driving around the storm and/or slowing down to wait out the storm and afterwards speeding up to arrive with minimum delay costs.

3. Cost function forms can affect both speed and vessel path and help in strategical decision making. The different functions can be altered to fit customers and are presented on a general basis for this study. It is found to be an

efficient way of manipulation behaviour, but it should be handled with care due to its effect on operational performance.

4. Several simulated voyages suggested routes stretching up to the north of the Bering Sea, which is most likely not realistic for the time period in question due to statistically rougher wave climate and occurrence of sea ice.
   Recommendation: A statistical and/or risk based model that include risk of sea ice occurrence, harsh weather in arctic areas, potential loss of communication and damaged goods.

Bibliography

Amaran, S., Sahinidis, N. V., Sharda, B. & Bury, S. J. (2014), 'Simulation optimization: a review of algorithms and applications', *Annals of Operations Research* **240**(1), 351–380.

Amdahl, J., Endal, A., Fuglerud, G., Hultgreen, L. R., Minsaas, K., Rasmussen, M., Sillerud, B., Sortland, B. & Valland, H. (2013), *TMR4105 Marin Teknikk Grunnlag*, NTNU, Trondheim.

Aydin, N., Lee, H. & Mansouri, S. A. (2017), 'Speed optimization and bunkering in liner shipping in the presence of uncertain service times and time windows at ports', *European Journal of Operational Research* **259**(1), 143–154.
URL: *http://dx.doi.org/10.1016/j.ejor.2016.10.002*

Bassam, A. M., Phillips, A. B., Turnock, S. R. & Wilson, P. A. (2015), 'Ship voyage energy efficiency assessment using ship simulators', *VI International Conference on Computational Methods in Marine Engineering MARINE 2015* **i**, 591–604.

Bouman, E. A., Lindstad, E., Rialland, A. I. & Strømman, A. H. (2017), 'State-of-the-art technologies, measures, and potential for reducing GHG emissions from shipping – A review', *Transportation Research Part D: Transport and Environment* **52**, 408–421.
URL: *http://dx.doi.org/10.1016/j.trd.2017.03.022*

Brockhaus, G. T. (2011), 'Hydrodynamic Design of Ship Bulbous Bows Considering Seaway and Operational Conditions', (September 2010), 1–191.

Choi, B. K. & Kang, D. (2013), *Modeling and Simulation of Discrete-Event systems*, Vol. 136.

Christiansen, M., Fagerholt, K., Nygreen, B. & Ronen, D. (2013), 'Ship routing and scheduling in the new millennium', *European Journal of Operational Research* **228**(3), 467–483.
URL: *http://dx.doi.org/10.1016/j.ejor.2012.12.002*

Dariusz, E. F. (2018), ShipX Vessel Responses (VERES) User´s Manual, Technical Report October, SINTEF Ocean AS.

DNV GL (2017), DNVGL-RP-C205: Environmental Conditions and Environmental Loads, Technical Report August.

Eide, M. S., Dals{\o}ren, S. B., Endresen, Ø., Samset, B., Myhre, G., Fuglestvedt, J. & Berntsen, T. (2013), 'Reducing CO2 from shipping - do non-CO2 effects matter', *Atmospheric Chemistry and Physics* **13**(8), 4183–4201.
URL: *https://www.atmos-chem-phys.net/13/4183/2013/*

Erikstad, S. O., Grimstad, A., Johnsen, T. & Borgen, H. (2015), 'VISTA (Virtual sea trial by simulating complex marine operations): Assessing vessel operability at the design stage', **1**(May), 107–123.

European Centre for Medium-Range Weather Forecast (2018).
URL: *https://apps.ecmwf.int/data-catalogues/era5/?class=ea*

Faltinsen, O. M. M. (1990), *Sea loads on ships and offshore structures.*

Fathi, D. E., Grimstad, A., Johnsen, T. A., Nowak, M. P. & Stalhane, M. (2013), 'Integrated decision support approach for ship design', *OCEANS 2013 MTS/IEEE Bergen: The Challenges of the Northern Dimension* .

Fischer, A., Nokhart, H., Olsen, H., Fagerholt, K., Rakke, J. G. & Stålhane, M. (2016), 'Robust planning and disruption management in roll-on roll-off liner shipping', *Transportation Research Part E: Logistics and Transportation Review* **91**, 51–67.
URL: *http://dx.doi.org/10.1016/j.tre.2016.03.013*

Hassani, V., Simon Sadjina NTNU SeverinSadjina, S., Alesund, N., og Romsdal, M., Stian Skjong NTNU StianSkjong, N., Trondheim, N. & Dariusz Fathi, N. (2016), 'Virtual Prototyping of Maritime Systems and Operations (ViProMa)', (June).

Hasselaar, T. W. F. (2011), An investigation into the development of an advanced ship performance monitoring and analysis system, PhD thesis.

Holtrop, J. & Mennen, G. G. J. (1982), 'An Approximate Power Prediction Method'.
URL: *http://papers.sae.org/971010/*

IMO (2011), Note by International Maritime Organization, Technical report.

IMO (2018), 'IMO'.
URL: *http://www.imo.org/en/About/Pages/Default.aspx*

Jalkanen, J. P., Brink, A., Kalli, J., Pettersson, H., Kukkonen, J. & Stipa, T. (2009), 'A modelling system for the exhaust emissions of marine traffic and its application in the Baltic Sea area', *Atmospheric Chemistry and Physics* **9**(23), 9209–9223.

Janssen, P. A. & Bidlot, J. R. (2018), 'Progress in Operational Wave Forecasting', *Procedia IUTAM* **26**, 14–29.
URL: *https://doi.org/10.1016/j.piutam.2018.03.003*

Jia, H., Adland, R., Prakash, V. & Smith, T. (2017), 'Energy efficiency with the application of Virtual Arrival policy', *Transportation Research Part D: Transport and Environment* **54**(July 2011), 50–60.
URL: *http://dx.doi.org/10.1016/j.trd.2017.04.037*

Journèe, J. M. J. (1976), Prediction of Speed and Behaviour of a Ship in a Sea-Way, Technical report, Technische Hogeschool Delft.

Kwon, Y. J. (2008), 'Speed loss due to added resistance in wind and waves', *The Naval Architect* pp. 14–16.

Li, C., Qi, X. & Song, D. (2016), 'Real-time schedule recovery in liner shipping service with regular uncertainties and disruption events', *Transportation Research Part B: Methodological* .

Lindstad, E. (2018), Alternative Fuels versus Traditional Fuels in Shipping - SOME.

Lindstad, E. & Bø, T. I. (2018), 'Potential power setups, fuels and hull designs capable of satisfying future EEDI requirements', *Transportation Research Part D: Transport and Environment* **63**(June 2018), 276–290.
URL: *https://doi.org/10.1016/j.trd.2018.06.001*

Lindstad, H., Asbjørnslett, B. E. & Jullumstrø, E. (2013), 'Assessment of profit, cost and emissions by varying speed as a function of sea conditions and freight market', *Transportation Research Part D: Transport and Environment* **19**, 5–12.
URL: *http://dx.doi.org/10.1016/j.trd.2012.11.001*

Lu, R., Turan, O., Boulougouris, E., Banks, C. & Incecik, A. (2015), 'A semi-empirical ship operational performance prediction model for voyage optimization towards energy efficient shipping', *Ocean Engineering* **110**(July 2014), 18–28.
URL: *http://dx.doi.org/10.1016/j.oceaneng.2015.07.042*

NORFORSK (1987), *Assessment of Ship Performance in a Seaway.*

Perera, L. P. & Soares, C. G. (2017), 'Weather routing and safe ship handling in the future of shipping', *Ocean Engineering* **130**, 684–695.

Prpić-Oršić, J. & Faltinsen, O. M. (2012), 'Estimation of ship speed loss and associated CO2emissions in a seaway', *Ocean Engineering* **44**, 1–10.

Prpić-Oršić, J., Vettor, R., Faltinsen, O. M. & Guedes Soares, C. (2016), 'The influence of route choice and operating conditions on fuel consumption and CO2emission of ships', *Journal of Marine Science and Technology (Japan)* **21**(3), 434–457.

Sandvik, E., Asbjørnslett, B. E. & Steen, S. (2018), 'Estimation of fuel consumption using discrete-event simulation - a validation study'.

Sandvik, E., Nielsen, J. B., Asbjørnslett, B. E., Pedersen, E. & Fagerholt, K. (n.d.), Scenario modelling for operational performance estimation (not published).

Sargent, R. G. (1981), An assessment procedure and a set of criteria for use in the evalutaion of computerized models and computer-based modeling tools. Final Technical Report RADDC-TR-80-409, Technical report, U. S. Air Force.

Sargent, R. G. (2004), Validation And Verification Of Simulation Models, *in* 'Winte Simulation Conference'.

Schlesinger, S., Crosbie, R. E., Gagné, R. E., Innis, G. S. & Lalwani, C. S. (1979), 'Terminology for model credibility', *SAGE* .

Serani, A., Leotardi, C., Iemma, U., Campana, E. F., Fasano, G. & Diez, M. (2016), 'Parameter selection in synchronous and asynchronous deterministic particle swarm optimization for ship hydrodynamics problems', *Applied Soft Computing Journal* .

SFI Smart Maritime - WP 4 (2019).
URL: *http://www.smartmaritime.no/work-packages/wp-4-ship-system-integration-and-validation/*

Skjong, S., Rindarøy, M., Kyllingstad, L. T., Æsøy, V. & Pedersen, E. (2017), 'Virtual prototyping of maritime systems and operations: applications of distributed co-simulations', *Journal of Marine Science and Technology (Japan)* **0**(0), 1–19.
URL: *http://dx.doi.org/10.1007/s00773-017-0514-2*

Smith, T. W. P., Jalkanen, J. P., Anderson, B. A., Corbett, J. J., Faber, J., Hanayama, S., O'Keeffe, E., Parker, S., Johansson, L., Aldous, L., Raucci, C., Traut, M., Ettinger, S., Nelissen, D., Lee, D. S., Ng, S., Agrawal, A., Winebrake, J. J. & Hoen, M., A. (2014), 'Third IMO Greenhouse Gas Study 2014', *International Maritime Organization (IMO) London, UK* .

Steen, S. (2014*a*), 'Experimental Methods in Marine Hydrodynamics', *NTNU* (August).

Steen, S. (2014*b*), *Motstand og propulsjon, propell og foilteori : kompendium*, Vol. UK-2014-99.

Steen, S. & Minsaas, K. (2014), *TMR4220 Naval Hydrodynamics Ship Resisance.*

Stopford, M. (2009), *Maritime Economics, Third Edition.*

Tillig, F., Ringsberg, J. W., Mao, W. & Ramne, B. (2018), 'Analysis of uncertainties in the prediction of ships' fuel consumption–from early design to operation conditions', *Ships and Offshore Structures* **13**, 13–24.

Vettor, R. & Guedes Soares, C. (2015), 'Detection and Analysis of the Main Routes of Voluntary Observing Ships in the North Atlantic', *Journal of Navigation* **68**(2), 397–410.

Vettor, R. & Guedes Soares, C. (2016), 'Rough weather avoidance effect on the wave climate experienced by oceangoing vessels', *Applied Ocean Research* **59**, 606–615. **URL:** *http://dx.doi.org/10.1016/j.apor.2016.06.004*

Wang, Z., Xia, L., Wang, Y. & Liu, L. (2014), 'Multiagent and Particle Swarm Optimization for Ship Integrated Power System Network Reconfiguration', *Mathematical Problems in Engineering* .

Zaccone, R., Ottaviani, E., Figari, M. & Altosole, M. (2018), 'Ship voyage optimization for safe and energy-efficient navigation: A dynamic programming approach', *Ocean Engineering* .

Zhang, B. J. & Zhang, S. L. (2018), *Research on ship design and optimization based on simulation-based design (SBD) technique.*

Appendix

Model VS full-scale data

Model VS full-scale data In Chapter 10 the operational parameters for fixed sailing calculation from Shanghai to Seattle is displayed. In **??** a summation of mean operational parameters are listed. In Chapter 10 the operational parameters for fixed sailing calculations from Shanghai to Panama is displayed. In Chapter 10 OD and Fixed calculations are compared for Shanghai Seattle. For OD comparison to Fixed for Shanghai Panama see Table 6.3.2.

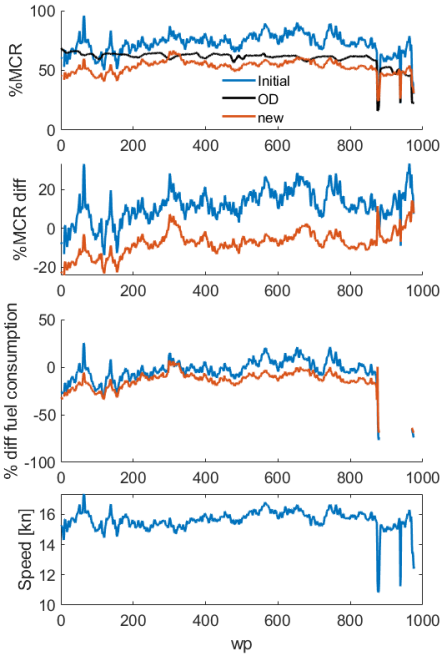

(a) Operational parameters Shanghai Seattle

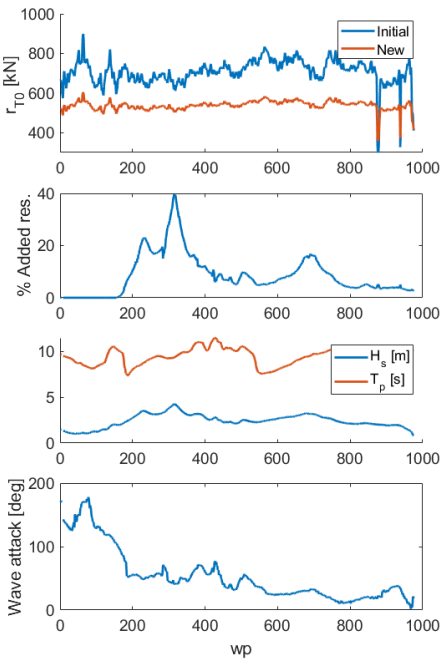

(b) Weather and resistance Shanghai Seattle

Operational parameters for fixed sailing calculations from Shanghai to Seattle

Mean and standard deviation propulsion power and fuel consumption for fixed route comparison

Route		Initial model			Corrected model		
		mean diff. power	std	mean diff f_c	mean diff. power	std	mean diff f_c
To	From	[%MCR]		[%MCR]	[%]		[%]
Shanghai	Seattle	11,9	± 7,9	-3,2	-7,3	± 5,9	-13,4
Shanghai	Panama	3,4	± 9,3	-12,9	-7,7	± 6,9	-14,8

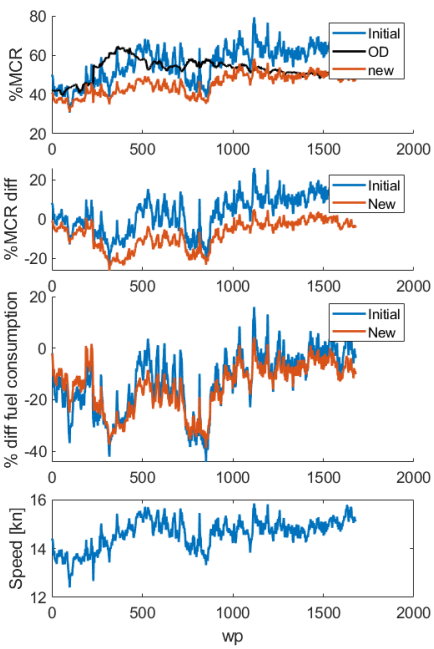

(a) Operational parameters Shanghai Panama

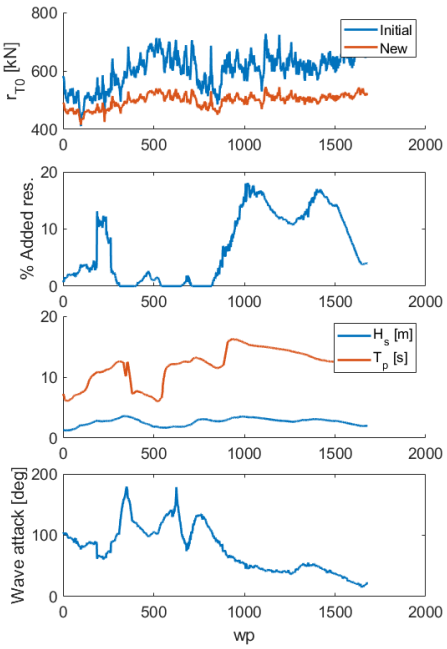

(b) Weather and resistance Shanghai Panama

Operational parameters for fixed sailing calculations from Shanghai to Panama

Full-scale data compared to fixed calculation with ship model from Shanghai to Seattle

Case	Distance [nm]	Duration [h]	Average speed [kn]	mean %MCR [%]	std [%]	Fuel consumption [ton]	Fuel con. rate [ton/day]	mean Hs [m]
OD	4010	257	15,7	82,6	1,7	337	32	2,4
Fixed	4010	257	15,7	53,1	5,5	296	29	2,4

Target speed and linear delay cost

Target time and linear delay cost In this study the target time and linearly increasing delay cost with rate κ is studied.

Shanghai Panama

Shanghai Panama Below the result for Shanghai Panama is presented

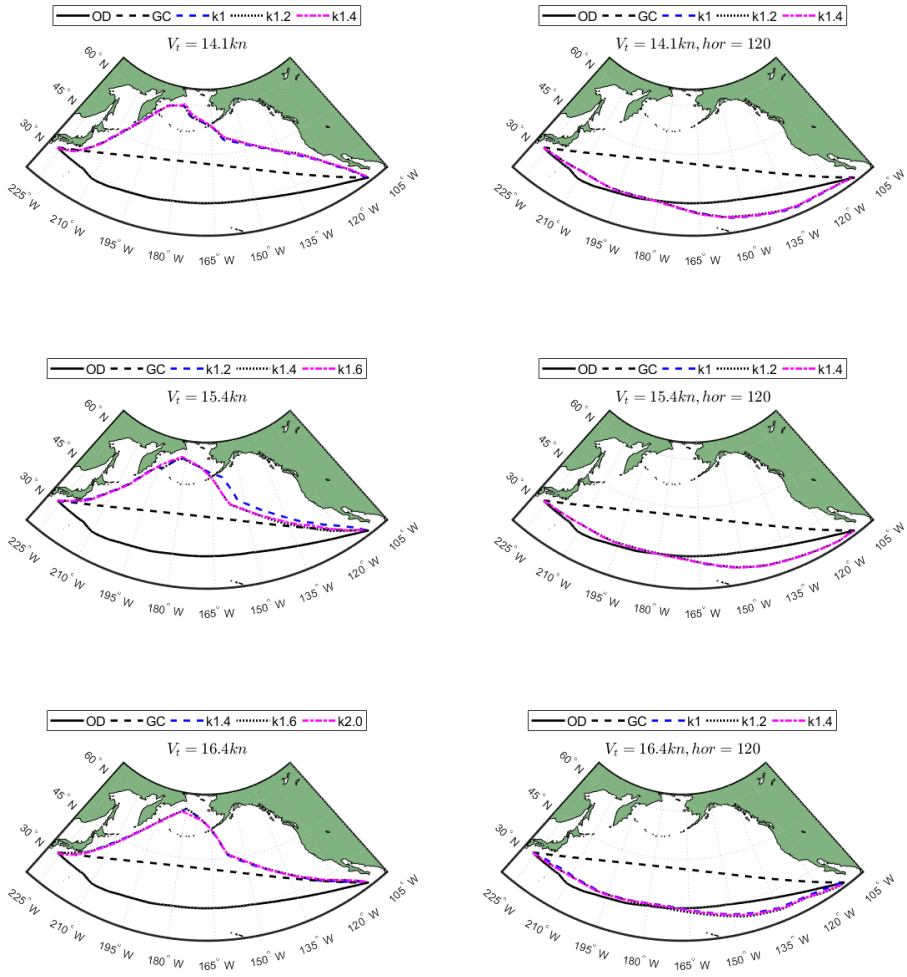

Voyage routing for varying speed and linear slope value κ. On the right horizon of 72 hours is disaplyd and on the left horizon of 120 hours are displayd

vt14.1

Scenario result overview for original linear kappa study vt 14.1 hor 72 hours

Case vt14.1	Distance [nm]	Duration [h]	Average speed [kn]	mean %MCR [%]	std [%]	Fuel consumption [ton]	Fuel con. rate [ton/day]	mean Hs [m]
k1	6377	468	13,6	45,2	14,4	492	25	3,0
k1.2	6382	456	14,0	48,0	16,6	507	27	3,1
k1.4	6407	450	14,2	50,1	18,5	522	28	3,1

Scenario result overview for original linear kappa study vt 14.1 hor 120 hours

Case vt14.1	Distance [nm]	Duration [h]	Average speed [kn]	mean %MCR [%]	std [%]	Fuel consumption [ton]	Fuel con. rate [ton/day]	mean Hs [m]
k1	6090	420	14,5	45,1	7,9	440	25	2,7
k1.2	6078	414	14,7	46,5	7,5	447	26	2,7
k1.4	6168	420	14,7	46,5	8,0	453	26	2,7

vt15.4

Scenario result overview for original linear kappa study vt 15.4 hor 72 hours

Case vt15.4	Distance [nm]	Duration [h]	Average speed [kn]	mean %MCR [%]	std [%]	Fuel consumption [ton]	Fuel con. rate [ton/day]	mean Hs [m]
k1.2	6385	438	14,6	55,9	15,4	560	31	3,6
k1.4	6389	432	14,8	57,3	16,3	567	32	3,6
k1.6	6408	432	14,8	57,2	16,7	568	32	3,6

Scenario result overview for original linear kappa study vt 15.4 hor 120 hours

Case vt15.4	Distance [nm]	Duration [h]	Average speed [kn]	mean %MCR [%]	std [%]	Fuel consumption [ton]	Fuel con. rate [ton/day]	mean Hs [m]
k1.2	6126	384	16,0	55,0	8,8	486	30	2,7
k1.4	6132	384	16,0	55,2	8,6	488	31	2,7
k1.6	6144	384	16	55,4	8,0	489	31	2,7

vt16.4

Scenario result overview for original linear kappa study vt 16.4 hor 72 hours

Case vt16.4	Distance [nm]	Duration [h]	Average speed [kn]	mean %MCR [%]	std [%]	Fuel consumption [ton]	Fuel con. rate [ton/day]	mean Hs [m]
k1.4	6386	432	14,8	57,1	17,0	568	32	3,7
k1.6	6407	432	14,8	58,8	17,4	584	32	3,8
k2	6426	420	15,3	62,2	19,3	601	34	3,8

Scenario result overview for original linear kappa study vt 16.4 hor 120 hours

Case vt16.4	Distance [nm]	Duration [h]	Average speed [kn]	mean %MCR [%]	std [%]	Fuel consumption [ton]	Fuel con. rate [ton/day]	mean Hs [m]
k1.4	6087	366	16,6	60,0	10,5	504	33	2,7
k1.6	6048	360	16,8	61,7	10,5	510	34	2,7
k2	6089	360	17,0	63,2	11,3	522	35	2,7

Further increased linear delay cost

To test if increased κ in calm seas do not affect operational parameters noticeably, κ increased up to 2.6. for route Shanghai Panama with target speed 15.4 knots and horizon of 120 hours.

Scenario result overview linear κ increase study for vt15.4 shanghai Panama

Case vt15.4	Distance [nm]	Duration [h]	Average speed [kn]	mean %MCR [%]	std [%]	Fuel consumption [ton]	Fuel con. rate [ton/day]	mean Hs [m]
k1.8	6132	384	16,0	55,3	7,8	489	31	2,7
k2.0	6149	384	16,0	55,3	7,6	489	31	2,7
k2.2	6132	384	16,0	55,5	7,5	490	31	2,7
k2.4	6148	384	16,0	55,2	8,9	488	31	2,7
k2.6	6154	384	16,0	55,3	7,5	489	31	2,7

Shanghai Seattle

Shanghai Seattle Below the results for Shanghai Seattle is presented

Scenario result overview for original linear kappa study vt 13.8 hor 120 hours for Shanghai Seattle

Case vt13.8	Distance [nm]	Duration [h]	Average speed [kn]	mean %MCR [%]	std [%]	Fuel consumption [ton]	Fuel con. rate [ton/day]	mean Hs [m]
k1	3324	240	13,9	39,2	5,2	220	22	1,9
k1.2	3330	240	13,9	39,3	4,7	221	22	1,9
k1.4	3330	240	13,9	39,3	5,8	221	22	1,8

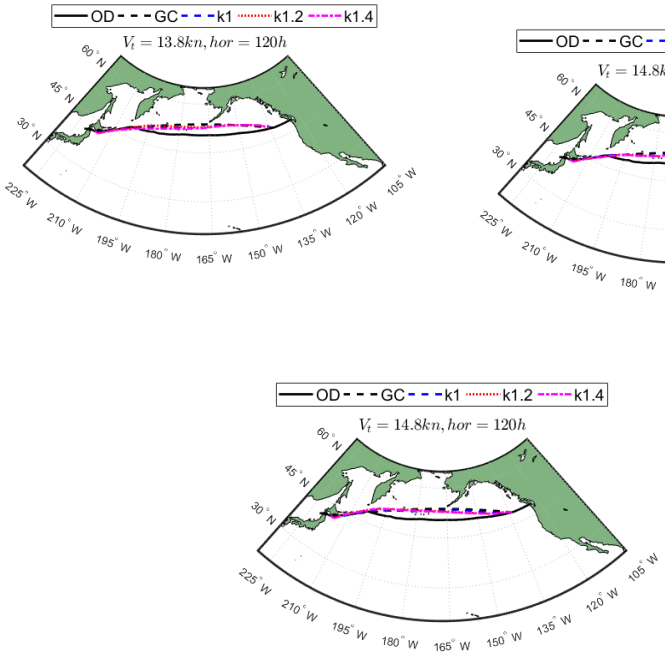

Voyage routing for varying speed and linear slope value κ for Shanghai Seattle

Scenario result overview for original linear kappa study vt 14.8 kn, hor 120 hours for Shanghai Seattle

Case vt14.8	Distance [nm]	Duration [h]	Average speed [kn]	mean %MCR [%]	std [%]	Fuel consumption [ton]	Fuel con. rate [ton/day]	mean Hs [m]
k1	3360	234	14,6	42,2	7,1	230	24	1,9
k1.2	3330	228	14,6	43,9	10,0	233	25	1,9
k1.4	3378	228	14,8	45,6	11,5	241	25	2,0

Scenario result overview for original linear kappa study vt 15.7 kn, hor 120 hours for Shanghai Seattle

Case vt15.7	Distance [nm]	Duration [h]	Average speed [kn]	mean %MCR [%]	std [%]	Fuel consumption [ton]	Fuel con. rate [ton/day]	mean Hs [m]
k1	3360	234	14,4	42,1	7,7	230	24	1,9
k1.2	3360	228	14,7	45,3	10,3	240	25	2,0
k1.4	3420	228	15,0	47,4	11,0	251	26	2,1

Computational Time

Vt [kn]	hor [h]	kappa [ton]	Cost func.	Distance GC [nm]	Way points [-]	Sim. time [h]	Sim. time per way point [s/wp]
14.1	72	1.0	y0	6211	1873	7.27	13.98
14.1	72	1.2	y0	6211	1825	7.19	14.17
14.1	72	1.4	y0	6211	1801	7.29	14.58
15.4	72	1.2	y0	6211	1753	10.24	21.04
15.4	72	1.4	y0	6211	1729	6.81	14.18
15.4	72	1.6	y0	6211	1729	6.73	14.00
16.4	72	1.4	y0	6211	1729	9.94	20.70
16.4	72	1.6	y0	6211	1729	6.98	14.54
16.4	72	2.0	y0	6211	1681	6.81	14.59
14.1	120	1.0	y0	6211	1681	11.51	24.65
14.1	120	1.2	y0	6211	1657	9.77	21.23
14.1	120	1.4	y0	6211	1681	11.05	23.65
15.4	120	1.2	y0	6211	1537	10.75	25.17
15.4	120	1.4	y0	6211	1537	8.61	20.17
15.4	120	1.6	y0	6211	1537	10.07	23.59
16.4	120	1.4	y0	6211	1465	9.88	24.28
16.4	120	1.6	y0	6211	1441	8.47	21.16
16.4	120	2.0	y0	6211	1441	9.09	22.72
15.4	48	1.2	y0	6211	1753	12.47	25.61
15.4	96	1.2	y0	6211	1801	7.02	14.03
15.4	102	1.2	y0	6211	1537	5.12	12.00
15.4	108	1.2	y0	6211	1537	4.57	10.71
15.4	114	1.2	y0	6211	1537	4.74	11.10
15.7	48	1.4	y0	3554	889	4.19	16.97
15.7	72	1.4	y0	3554	889	3.65	14.77
15.7	96	1.4	y0	3554	913	3.31	13.05
15.7	120	1.4	y0	3554	913	3.59	14.14
13.8	120	1.2	y0	3554	961	3.19	11.96
13.8	120	1.4	y0	3554	961	3.30	12.36
13.8	120	1.6	y0	3554	961	3.48	13.03
14.8	120	1.2	y0	3554	937	6.78	26.04
14.8	120	1.4	y0	3554	913	4.36	17.17
14.8	120	1.6	y0	3554	913	3.89	15.36
15.7	120	1.2	y0	3554	937	6.56	25.22
15.7	120	1.4	y0	3554	913	4.29	16.91
15.7	120	1.6	y0	3554	913	3.72	14.68
14.1	120	1.0	y1	6211	1681	10.67	22.85
14.1	120	1.0	y2	6211	1657	5.77	12.53
14.1	120	1.0	y3	6211	1681	10.47	22.43
14.1	120	1.0	y4	6211	1657	10.79	23.44
14.1	96	1.0	y1	6211	1849	11.06	21.54
14.1	96	1.0	y2	6211	1657	6.76	14.68
14.1	96	1.0	y3	6211	1825	6.27	12.38
14.1	96	1.0	y4	6211	1657	6.58	14.30
						Average [s/wp]:	17.92
						Std:	4.86

The attached zip file contains the following:

1. Poster
2. Table look-up generation code from MATLAB for preprocessing data before simulation

Carita Gyldenskog Ranvik

NTNU
Norwegian University of
Science and Technology